University of São Paulo
"Luiz de Queiroz" College of Agriculture

Mechanistic numerical modeling of solute uptake by plant roots

Andre Herman Freire Bezerra

Thesis presented to obtain the degree of Doctor of Science. Area: Agricultural Systems Engineering

Piracicaba
2015

Andre Herman Freire Bezerra
Bachelor in Agronomy

Mechanistic numerical modeling of solute uptake by plant roots

Advisor:
Prof. Dr. **QUIRIJN DE JONG VAN LIER**

Thesis presented to obtain the degree of Doctor of Science. Area: Agricultural Systems Engineering

Piracicaba
2015

To the past,

to the present, and

to the future

ACKNOWLEDGEMENT

Agradeço aos meus amigos e colegas de pós-graduação pelas longas horas de discussão e convivência.

Ao Conselho Nacional de Densenvolvimento Científico e Tecnológico (CNPq) pela bolsa de doutorado e à Coordenação de Aperfeiçoamento de Pessoal de Nível Superior (CAPES) pela bolsa de estágio *sandwich*.

Ao meu orientador Quirijn de Jong van Lier, pelas suas valiosas contribuições e inestimável suporte.

À minha noiva, Flávia, pelo apoio nesse fim de caminhada e início de uma outra jornada que iremos enfrentar juntos.

I also would like to thank my coleagues at the Wageningen University for all the support that, even without knowing, they gave me and specially to my advisors Sjoerd van der Zee (official), Jos van Dam and Peter de Willigen to every contribution for this work. Wihtout your support, this thesis would be still a project.

Some catch phrase that everyone expect to read.

CONTENTS

RESUMO

Modelagem numérica de extração de solutos pelas raízes

Uma modificação em um modelo existente de extração de água e transporte de solutos foi realizada com o objetivo de incluir nele a possibilidade de simular a extração de soluto pelas raízes. Uma solução numérica para a equação de convecção-dispersão (ECD), que utiliza um esquema de resolução completamente implícito, foi elaborada e considera o fluxo transiente de água e solutos com uma condição de contorno à superfície da raiz de extração de soluto dependente de sua concentração no solo, baseada na equação de Michaelis-Menten (MM). Uma aproximação linear para a equação de MM foi implementada de tal forma que a ECD tem uma solução linear e outra não-linear. O modelo considera uma raiz singular com geometria radial sendo sua superfície a condição de contorno (limite) de extração e sendo o limite extremo a meia-distância entre raízes vizinhas, função da densidade radicular. O modelo de transporte de soluto proposto inclui extração de soluto ativa e passiva e prediz a concentração de soluto como uma função do tempo e da distância à superfície da raiz, além de estimar a transpiração relativa da planta, que por sua vez afeta a extração de água e solutos e é relacionado com a condição de estresse da planta. Simulações mostram que as soluções linear e não-linear resultam em predições de extração de solutos significativamente diferentes quando a concentração de solutos no solo está abaixo de um valor limitante (C_{lim}). A redução da extração em baixas concentrações pode resultar em uma redução adicional na transpiração relativa. As contribuições ativa e passiva da extração de solutos variam com parâmetros relacionados à espécie de íon, à planta, à atmosfera e às propriedades hidráulicas do solo. O modelo apresentou uma boa concordância com um modelo analítico que aplica uma condição de contorno linear, à superfície da raiz, de extração de solutos dependente da concentração no solo. A vantagem do modelo numérico sobre o analítico é que ele permite simular fluxos transientes de água e solutos, sendo, portanto, possível simular uma maior gama de situações. Se faz necessário simulações com diferentes cenários e comparações com dados experimentais para se verificar a performance do modelo e, possivelmente, sugerir melhorias.

Palavras-chave: Transporte de solutos; Michaelis-Menten; Fluxo transiente de solutos

ABSTRACT

Mechanistic numerical modeling of solute uptake by plant roots

A modification in an existing water uptake and solute transport numerical model was implemented in order to allow the model to simulate solute uptake by the roots. The convection-dispersion equation (CDE) was solved numerically, using a complete implicit scheme, considering a transient state for water and solute fluxes and a soil solute concentration dependent boundary for the uptake at the root surface, based on the Michaelis-Menten (MM) equation. Additionally, a linear approximation was developed for the MM equation such that the CDE has a linear and a non-linear solution. A radial geometry was assumed, considering a single root with its surface acting as the uptake boundary and the outer boundary being the half distance between neighboring roots, a function of root density. The proposed solute transport model includes active and passive solute uptake and predicts solute concentration as a function of time and distance from the root surface. It also estimates the relative transpiration of the plant, on its turn directly affecting water and solute uptake and related to water and osmotic stress status of the plant. Performed simulations show that the linear and non-linear solutions result in significantly different solute uptake predictions when the soil solute concentration is below a limiting value (C_{lim}). This reduction in uptake at low concentrations may result in a further reduction in the relative transpiration. The contributions of active and passive uptake vary with parameters related to the ion species, the plant, the atmosphere and the soil hydraulic properties. The model showed a good agreement with an analytical model that uses a linear concentration dependent equation as boundary condition for uptake at the root surface. The advantage of the numerical model is it allows simulation of transient solute and water uptake and, therefore, can be used in a wider range of situations. Simulation with different scenarios and comparison with experimental results are needed to verify model performance and possibly suggest improvements.

Keywords: Solute transport; Michaelis-Menten; transient solute flux

LIST OF FIGURES

LIST OF TABLES

LIST OF ABREVIATIONS

CDE – Convection-dispersion equation

CU – Constant solute uptake model

LU – Linear solute uptake model

LCC – Limiting concentration condition

MM – Michaelis-Menten

ZU – Zero solute uptake model

NLU – Non-linear solute uptake model

SPA – Soil-plant-atmosphere

LUP – Linear uptake phase

CUP – Constant uptake phase

NUP – Non-linear uptake phase

LIST OF SYMBOLS

a_i – Tridiagonal matrix coefficient

b_i – Tridiagonal matrix coefficient

c_i – Tridiagonal matrix coefficient

f_i – Tridiagonal matrix coefficient

A_p – Plant area (m^2)

C – Solute concentration in soil water (mol cm^{-3})

C_0 – Solute concentration in soil water at the root surface (mol cm^{-3})

C_2 – Solute concentration threshold for active uptake (mol cm^{-3})

C_{ini} – Initial solute concentration in soil water (mol cm^{-3})

C_{lim} – Limiting solute concentration for potential solute uptake (mol cm^{-3})

C_{min} – Minimum solute concentration for zero uptake (mol cm^{-3})

C_s – Solute concentration in bulk soil (mol cm^{-3})

C_w – Differential water capacity (–)

CL – Solute concentration in soil water for linear model (mol cm^{-3})

CNL – Solute concentration in soil water for non-linear model (mol cm^{-3})

D – Effective diffusion-dispersion coefficient (m^2 s^{-1})

$D_{m,w}$ – Molecular diffusion coefficient in water (m^2 s^{-1})

D_s – Mechanical dispersion coefficient (m^2 s^{-1})

d_s – Soil density (g m^{-3})

dP – Increment quantity of model parameter in sensitivity analysis

dY – Response in model output when applied dP

F – Solute extraction equation (–)

H – Total hydraulic head (m)

H_{lim} – Limiting total hydraulic head (m)

h – Pressure head (m)

h_π – Osmotic head (m)

h_{lim} – Limiting pressure head (m)

h_g – Gravitational head (m)

I_m – Coefficient of Michaelis-Menten equation (plant solute demand) (mol m^{-2} s^{-1})

i – Segment position index (–)

j – Time step index (–)

k – Linear component of Michaelis-Menten equation for high concentrations (–)

K – Hydraulic conductivity (m s^{-1})

K_m – Coefficient of Michaelis-Menten equation (plant affinity to the solute type) (mol cm^{-3})

K_s – Saturated hydraulic conductivity (m s^{-1})

L – Root length (m)

m_s – Soil mass (g)

n – Empirical parameter of Van Genuchten (1980) equation (–, Section 3.3) or number of elements of the discretized domain (–, Section 4)

P – Model parameter in sensitivity analysis

p – Iteration level index (–)

q – Water flux density (m s^{-1})

q_0 – Water flux density at the root surface (m s^{-1})

q_s – Solute flux density (mol m^{-2} s^{-1})

q_{s0} – Solute flux density at the root surface (mol m^{-2} s^{-1})

R – Root length density (m m^{-3})

r – Distance from axial center (m)

r_0 – Root radius (m)

r_m – Half distance between roots (m)

S – Rate at which the segment size increases (–)

t – Time (s)

T_p – Potential transpiration (–)

T_r – Relative transpiration (–)

Y – Model output in sensitivity analysis

z – Rooted soil depth (m)

α – Empirical parameter of Van Genuchten (1980) equation (m^{-1}, Section 3.3) or active contribution to solute uptake (–, Section 3.5)

$\alpha(C)$ – Solute uptake shape function (–)

β – Passive uptake slope (m s^{-1})

Δr – Space step (m)

Δr_{max} – Maximum space step (m)

Δr_{min} – Minimum space step (m)

Δt – Time step (s)

δ – Difference between linear and non-linear models for concentration (mol cm^{-3}) and cumulative uptake (mol)

η – Relative partial sensitivity (–)

θ – Soil water content (m^3 m^{-3})

Θ – Effective saturation (–)

θ_r – Residual water content (m^3 m^{-3})

θ_s – Saturated water content (m^3 m^{-3})

λ – Empirical parameter of Van Genuchten (1980) equation (–)

τ – Solute dispersivity (m)

ψ – Active uptake slope (m s^{-1})

ξ – Tortuosity factor (–)

1 INTRODUCTION

Crop growth is directly related to plant transpiration, and the closer the cumulative transpiration over a growing season is to its potential value, the higher will be the crop yield. Any stress occurring during crop development results in stomata closure and transpiration reduction, affecting productivity. Therefore, knowing how plants respond to abiotic stresses like those related to water and salt, and predicting and quantifying them, is important not only to improve the understanding of plant-soil interactions, but also to propose better crop management practices. The interpretation of experimental data to analyze the combined water and salt stress on transpiration and yield has been shown to be difficult due to the great range of possible interactions between the factors determining the behavior of the soil-plant-atmosphere (SPA) system. Modeling has been shown to be an elucidative manner to analyze the involved processes and mechanisms, providing insight in the interaction of water and salt stress.

Analytical models describing transport of nutrients in soil towards plant roots usually consider steady state conditions with respect to water flow to deal with the high non-linearity of soil hydraulic functions. Several simplifications (assumptions) are needed regarding the uptake of solutes by the roots, most of them also imposed by the non-linearity of the influx rate function. Consequently, although analytical models describe the processes involved in transport and uptake of solutes, they are only capable of simulating water and solute flow just for specific boundary conditions. Therefore, applying these models in situations that do not exactly correspond to their boundary condition may lead to a rough approximation but may also result in erroneous predictions. Many of the available analytical solutions include special math functions (Bessels, Airys or infinite series, for example) that need, at some point, numerical algorithms to compute results. For the case of the convection-diffusion equation, even the fully analytical solutions are restricted by numerical procedures, although with computationally efficient and reliable results.

As a substitute to analytical solutions, numerical modeling allows more flexibility when dealing with non-linear equations, being an alternative to better cope with diverse boundary conditions. The functions can be solved considering transient conditions for water and solute flow but with some pullbacks regarding numerical stability and more processing to perform calculations. In general, numerical models use empirical functions

that relate osmotic stress to some electric conductivity of the soil solution. The parameters of these empirical models depend on soil, plant and atmospheric conditions in a range covered by the experiments used to generate data for model calibration. Using these models out of the measured range is not recommended and, in these cases, a new parameter calibration should be done. Physical/mechanistic models for the solute transport equations describe the involved processes in a wider range of situations since it is less dependent on experimental data, giving more reliable results.

The objective of this thesis is to present a modification of the model of root water uptake and solute transport proposed by De Jong van Lier, Van Dam and Metselaar (2009). This modification allows the model to take into account plant solute uptake. To do so, a numerical mechanistic solution for the equation of convection-dispersion will be developed that considers transient flow of water and solute, as well as root competition. A soil concentration dependent solute uptake function as boundary condition at the root surface was assumed. In this way, the new model allows prediction of active and passive contributions to the solute uptake, which can be used to separate ionic and osmotic stresses by considering solute concentration inside the plant. The proposed model is compared with the original model, with a constant solute uptake numerical model and with an analytical model that uses a steady state condition for water content.

2 LITERATURE REVIEW

2.1 Modeling solute transport and uptake by roots

Solute transport in soil and solute uptake by the plants have extensively been studied in the last half century. As a result, several simulation models have been developed to predict water and solute flows within the vadose zone. They are usually classified as microscopic or macroscopic, according to the considered scale (FEDDES; RAATS, 2004). Microscopic models (BARBER, 1974; CUSHMAN, 1979; DE WILLIGEN; VAN NOORDWIJK, 1994; ROOSE; FOWLER; DARRAH, 2001) consider a single cylindrical root, of uniform radius and absorption properties (GARDNER, 1965), that extracts water and solute by an axis-symmetric flow according to the defined boundary condition at the root surface. The water flow is described using the Richards equation and the solute flow using the convection-dispersion equation (CDE), both formulated in radial coordinates. The flow towards the root is driven by hydraulic head and concentration gradients between the root and the surrounding soil, proportional to the hydraulic conductivity and solute diffusivity. One of the advantages of the microscopic approach is that it implicitly simulates water uptake compensation, as the computed local water potential gradients control the uptake for the whole root system (ŠIMUNEK; HOPMANS, 2009). Despite the more realistic simulation of soil-root interactions, microscopic models require a large computational effort for the simulations and, therefore, are limited to applications of relatively small scale of a single plant. Chapter 3 shows, in more details, the theory of microscopic models.

Macroscopic models (ŠIMÙNEK; ŠEJNA; VAN GENUCHTEN, 2006; SOMMA; HOPMANS; CLAUSNITZER, 1998; VAN DAM et al., 2008) consider the whole root zone as a single uniform extraction component whereby the potential transpiration is distributed over the root zone and it is proportional to the rooting density. This approach neglects the effects of root geometry and flow pathways around individual roots, and considers water and solute uptakes as a sink term added to their respective mass balance equations. On the other hand, macroscopic models are able to simulate processes at the plot or field scale. They are sometimes incorporated in complete hydrological models that also deal with drainage, crop growth and productivity.

Another classification of models, relates to the experimental approach of the phenomenon, distinguishing between empirical and mechanistic models. Empirical models (CHANTER, 1981; ROSS, 1981; YEROKUN; CHRISTENSON, 1990) are based on

the response of a set of experiments and attempt to describe the observed phenomenon without hypothesizing about underlying mechanisms. They are usually of stochastic nature and have the advantage of being relatively simple, allowing to predict the results of the processes with a good certainty. The main disadvantage of this kind of model is that the model parameters do not have a clear physical, physiological or biological meaning, limiting interpretation and substantial model improvement. Furthermore, the application of these models is limited to boundary conditions corresponding to the experiments/observations that they were developed from, and they will probably lead to incorrect or inaccurate predictions in scenarios that were not used for their development. Mechanistic models (BARBER, 1974; CUSHMAN, 1979; DE WILLIGEN; VAN NOORDWIJK, 1994; ROOSE; FOWLER; DARRAH, 2001; ŠIMÙNEK; ŠEJNA; VAN GENUCHTEN, 2006; SOMMA; HOPMANS; CLAUSNITZER, 1998; VAN DAM et al., 2008) seek to explain the physical mechanisms that drive the phenomenon, requiring a better understanding and mathematical description of the underlying processes. Although the parameters may be difficult to measure, they have a physical meaning – they can be explained by the processes and their relationships, and they can be measured independently – and, therefore, can be adapted to be used in a broad variety of scenarios. Good reviews of available root solute uptake models can be found in Rengel (1993), Feddes and Raats (2004) and Silberbush, Eshel and Lynch (2013).

2.2 Solute mobility in soils

Solute mobility in soil is described by two processes: 1) convective transport by water mass flow through the transpiration stream, and 2) movement driven by diffusion that depends on the solute concentration gradient in the soil caused by depletion of solutes due to root uptake (BARBER, 1962). The first to recognize that solutes move towards the root due to the uptake process was Bray (1954). Since then, the efforts to describe the solute movement in soils were directed to develop analytical models and, when more computational means became available, numerical models. The earlier analytical solutions for the CDE were formulated considering a steady state condition to the water flow and a solute uptake governed by the solute concentration in the soil solution (BARBER, 1974, CUSHMAN, 1979, NYE; MARRIOTT, 1969) or determined by a constant plant demand (DE WILLIGEN, 1981). The concentration limiting (or supply driven) approach may overestimate the uptake in scenarios where solute supply to the root is not limiting (BARRACLOUGH; LEIGH, 1984) whilst the constant plant demand (or demand

driven) formulation may overestimate the uptake when the soil is very dry or at low solute concentration at the root surface, when the diffusive flow prevails. Later, Roose (2000) formulated analytical solutions for different conditions of uptake, considering a so called 'pseudo-steady state' condition for water flow and the interference of root hairs and mycorrhizae in the uptake process, offering also an analytical solution to upscaling from the single root to a three-dimensional root architecture uptake model.

Solute uptake can be described by the Michaelis-Menten (MM) equation (BARBER, 1995, BARBER; CUSHMAN, 1981, SCHRÖDER et al., 2012, ŠIMUNEK; HOPMANS, 2009) according to which uptake increases with increasing solute concentration asymptotically approaching maximum uptake (further details in Section 3.5). The necessary parameters are the MM constant (K_m), the maximum solute uptake (I_m) and the minimum solution concentration at which uptake ceases (C_{min}) (BARBER, 1995). Epstein and Hagen (1952) were the first to use the MM equation to represent the uptake of a solute and its concentration in external medium (for potassium and sodium solutions in barley roots) and it has been frequently used since then. The MM equation is supposed to describe well the solute uptake for both anions (EPSTEIN, 1972, SIDDIQI et al., 1990, WANG et al., 1993) and cations (BROADLEY et al., 2007; KELLY; BARBER, 1991; KOCHIAN; LUCAS, 1982; LUX et al., 2011; SADANA et al., 2005) in the low concentration range and, adding a linear component (k) to the equation, it can properly estimates the uptake rate also for higher concentrations (BORSTLAP, 1983; BROADLEY et al., 2007; EPSTEIN, 1972; KOCHIAN; LUCAS, 1982; VALLEJO; PERALTA; SANTA-MARIA, 2005; WANG et al., 1993). Many authors agree that for low concentration in external medium, the uptake is driven by an active plant mechanism, as it occurs contrary the solute gradient between root and soil (Epstein's mechanism I). For the high concentration range, solutes are freely transported from soil to roots by diffusion and occasional convection. This passive transport is known as Epstein's mechanism II (KOCHIAN; LUCAS, 1982; SIDDIQI et al., 1990). Moreover, experiments have shown that a minimum concentration (C_{min}) bellow which the uptake ceases is commonly found (DUDAL; ROY, 1995; MACHADO; FURLANI, 2004; MOUAT, 1983). Details on Epstein's mechanisms and its physiological mechanisms, as well as on active and passive uptake, are found in Epstein (1960) and Fried and Shapiro (1961).

The values of MM parameters are strongly dependent on the experimental methods used and vary with plant species, plant age, plant nutritional status, soil temperature and pH (BARBER, 1995, SHI et al., 2013). Therefore, they have to be determined for

each particular experimental scenario. Some types of experiments to determine the kinetic parameters I_m, K_m and C_{min} include hydroponically-grown plants (BARBER, 1995) and the use of radioisotopes to estimate them directly from soil (NYE; TINKER, 1977). The latter is more realistic since there is a large difference between a stirred nutrient solution and the complex and dynamic soil medium. Measuring C_{min} is particularly difficult (LAMBERS; CHAPIN III; PONS, 2008; SEELING; CLAASSEN, 1990) because it occurs at very low concentration levels that may be hard to be accurately measured. Seeling and Claassen (1990) show that C_{min} can be neglected for the cases of high K_m values.

There are other alternatives to describe the solute uptake rate function apart from the MM equation. Dalton, Raats and Gardner (1975) proposed a physical-mathematical model that includes active uptake, mass flow and diffusion, expressing solute uptake as being proportional to root water uptake. Bouldin (1989) described the uptake from low and high concentration solutions by two linear equations, thus simplifying the process of solute uptake at the root surface to two diffusion components (RENGEL, 1993). Tinker and Nye (2000) determined the uptake rate as a linear component followed by a constant rate phase where the threshold value is dependent on solute concentration inside the plant. Nevertheless, the MM equation is the most frequently used equation in root solute uptake models for being physically grounded and for its good agreement with experimental data.

Combined water and solute uptake models compute averages or local pressure and osmotic heads, allowing estimating plant water and osmotic stress. Feddes, Kowalik and Zaradny (1978) developed an empirical water stress model relating the actual transpiration to pressure head, originating a piecewise transpiration reduction function in which the potential transpiration decreases linearly according to threshold values of pressure head that account for excess or shortage of soil water. As the presence of solutes in the soil solution reduces the total hydraulic head – affecting root water uptake – the compound effect in transpiration reduction by water and salt stress are commonly supposed to be either additive or multiplicative. However, crops seem to respond to water and salt stress differently.

Shalhevet and Hsiao (1986) found that transpiration of cotton and pepper plants reduces more strongly under low pressure head than under an equivalent low osmotic head. Similar results have already been found by Sepaskhah and Boersma (1979) for wheat, and by Parra and Romero (1980) for beans. Thus, empirical weighting factors have been introduced in the transpiration reduction function to account for the different response of a crop to osmotic and pressure heads.

Some models treat the combined water and salt stress neither in an additive or in a multiplicative way. Homaee (1999) developed a piecewise reduction function similar to the Feddes, Kowalik and Zaradny (1978) and concluded that the function fitted his experimental data better than any additive or multiplicative model. De Jong van Lier, Van Dam and Metselaar (2009) proposed a microscopic analytical model to estimate relative transpiration as a function of soil and plant parameters. Their mechanistic approach reduces the need of empirical parameters and does not require any explicit assumption (additive or multiplicative) to derive the combined water and salt stress. Results show good agreement with experimental data, although some discrepancies exist, especially under wet conditions. Their model does not consider root solute uptake. Considering root solute uptake would interfere in solute concentrations estimative, leading to more realistic simulations and to a better prediction of the crop response to the combined water and osmotic stress.

3 THEORETICAL FRAMEWORK

This chapter focuses on the theoretical aspects used in the methodology. It briefly describes the Richards equation that is applied in water flow models and details the convection-dispersion equation for solute transport. Both flow models are described with emphasis on the microscopic approach. Also, a short explanation about the Michaelis-Menten kinetics for nutrient uptake is given.

3.1 Microscopic approach

As mentioned in the previous chapter, models for water and solute uptake can be divided in macroscopic and microscopic ones. The model developed in this thesis is microscopic, and we will present the basic theory behind it.

Microscopic root uptake models consider a single cylindrical root of radius r_0 (m) with an extraction zone being represented by a concentric cylinder of radius r_m (m) that bounds the half-distance between roots. The height of both cylinders is z (m) and represents the rooted soil depth. The basic assumptions of this type of model is that the root density does not change with depth and there is no difference in intensity of extraction along the root surface. Water and solute flows are axis-symmetric.

It is common to report root length density R (m m^{-3}) and r_0. These are related to r_m and root length L (m) by the following equations:

$$r_m = \frac{1}{\sqrt{\pi R}} \tag{1}$$

$$L = \frac{A_p z}{\pi {r_m}^2} \tag{2}$$

where A_p (m^2) is the soil surface area occupied by the plant. For the case that there is no available data from literature, one can obtain the value of L from relatively simple measurements of root and soil characteristics as soil mass (m_s, kg) and density (d_s, kg m^{-3}), and root average radius ($\overline{r_0}$, m)

$$L = \frac{d_s A_p z - m_s}{d_s \pi \overline{r_0}^2} \tag{3}$$

allowing to estimate r_m by

$$r_m = \sqrt{\frac{A_p z}{\pi L}} \tag{4}$$

and R by

$$R = \frac{1}{\pi {r_m}^2}\,. \tag{5}$$

A complete derivation of the Equations (1) to (5) is given in Appendix A. The water and solute flow equations in microscopic models are, likewise, presented in radial coordinates. The following sections deal with those equations and their corresponding boundary conditions.

3.2 Water flow equation

The equation for water flow for a homogeneous and isotropic soil, in saturated and non-saturated conditions, is given by the Richards equation. In radial coordinates, it can be written as:

$$r\frac{\partial\theta}{\partial t} = -\frac{\partial q}{\partial r} \tag{6}$$

where r (m) is the distance from the root axial center, θ (m^3 m^{-3}) is the water content in soil and t (s) is the time. The water flux density q (m s^{-1}) is given by the Darcy-Buckingham equation:

$$q = -K(\theta)\frac{dH}{dr} \tag{7}$$

where K (m s^{-1}) is the soil hydraulic conductivity and H is the total hydraulic potential. This equation describes the axis-symmetric laminar water flux for (un)saturated soil.

The substitution of Equation (7) into (6) results in a second-order partial differential equation and, therefore, initial and boundary conditions are required to yield a particular solution. The most commonly employed initial condition is of constant water content or pressure head along the radial distance, although a function of water content (or pressure head) over distance can also be used. In analytical solutions, a steady state condition with respect to water flow is often used to solve the equation. The high non-linearity of the hydraulic functions (see Section 3.3) makes a transient solution rather complex and, sometimes, impractical. In numerical solutions, on the other hand, it is easy to define a transient water flow condition, allowing more realistic simulations. Boundaries for both steady state and transient solutions can be either of pressure head or water flux, as shown in Equations (8) and (9) respectively:

$$h(r_i, t) = f(t) \tag{8}$$

$$K(\theta)\frac{\partial h}{\partial r}\bigg|_{r=r_i} = g(t) \tag{9}$$

where $f(t)$ and $g(t)$ is a constant or a time variable function of pressure head and water flux, respectively; and r_i is the distance from axial center to the specific boundary. In the case of microscopic models, r_i can assume values of distance from axial center to root

surface (inner boundary) and to the end of the domain (outer boundary). Macroscopic models use the Cartesian coordinate system and, for one-dimension, represent the domain along the z-axis (depth) instead of r. Thus, z_i values would be of the distance from the soil surface (top boundary) to a certain depth, *e.g.* root depth (bottom boundary).

In most microscopic models, the boundary conditions are of flux type, according to Equation (9). At the root surface, flux times area is supposed to match transpiration, and at the outer boundary, a zero flux is often assumed – meaning inter-root competition for water. Therefore, the only water exit is at the root surface through the transpiration stream. In macroscopic models that deal with the entire root zone, both boundary types are equally found, depending on the simulation scenario to consider (soil surface evaporation, irrigation or rain, presence of water table, drainage, water root uptake, etc.). A sink-source term is then added to Equation (6) to deal with such water inputs and outputs (as seen in the previous chapter).

The hydraulic potential H is composed of pressure (h) and gravitational (h_g) heads in models that do not consider the presence or flow of solutes. In order to deal with solutes, the osmotic head (h_π) is added to H and its value is calculated through the solute transport equation, detailed in Section 3.4. In microscopic models, h_g is often neglected due to its minor relevance.

3.3 Soil hydraulic functions

The soil hydraulic properties K, θ and h are interdependent and, as mentioned in the previous section, their relation is highly non-linear. Among available models to describe soil hydraulic properties, the Van Genuchten (1980) equation system is frequently used:

$$\theta(h) = \theta_r + \frac{\theta_s - \theta_r}{[1 + |\alpha h|^n]^{1-(1/n)}} \tag{10}$$

$$K(\theta) = K_s \Theta^\lambda [1 - (1 - \Theta^{n/(n-1)})^{(1-(1/n))}]^2 \tag{11}$$

where Θ (–) is the effective saturation defined by $\frac{(\theta-\theta_r)}{(\theta_s-\theta_r)}$; θ_s ($m^3\ m^{-3}$) and θ_r ($m^3\ m^{-3}$) are the saturated and residual water contents, respectively; and α (m^{-1}), λ (–) and n (–) are empirical parameters.

Equation (11) was developed by Van Genuchten (1980) considering the Mualem (1976) theory on relative unsaturated hydraulic conductivity. Parameter n appears in

both Equations (10) and (11) and can be determined from a water retention experiment. In doing so, the only unknown parameter of the K-θ relation that remains is the λ parameter, which needs experimental verification to obtain the K function.

3.4 Solute transport

Solute transport in soils occurs by diffusion and convection and can be described by the convection-diffusion equation. In radial coordinates, it can be written as:

$$r\frac{\partial(\theta C)}{\partial t} = -\frac{\partial q_s}{\partial r} \tag{12}$$

where C (mol cm^{-3}) is the concentration of solute in soil solution. The solute flux density q_s (mol m^{-2} s^{-1}) is given by:

$$q_s = -D(\theta)\frac{dC}{dr} + qC \tag{13}$$

where D (m^2 s^{-1}) is the effective diffusion-dispersion coefficient. This equation describes the solute flux in the soil solution. The convective flux is accounted for by the second term on the right-hand side of the equation (13) and the diffusive-dispersive flux by the first term.

Transport by convection occurs due to the movement of diluted solutes carried by mass flow of water proportional to the solute concentration in soil solution. It is noticeable that the convective contribution to solute flux reduces as water flux q becomes small, therefore the convective flux is highly dependent on water content gradients and hydraulic conductivity. Convection also affects the solute flow due to a water velocity gradient originated in the micropore space of the soil. As solutes are carried with different velocities, a concentration gradient develops, allowing a diffusive movement within this micropore space. This microscale process is called mechanical dispersion and can be expressed by macroscopic variables as:

$$D_s = \tau\frac{q}{\theta} \tag{14}$$

where D_s (m^2 s^{-1}) is the mechanical dispersion coefficient, τ (m) is the dispersivity and the relation q/θ (m s^{-1}) accounts for the average pore water velocity.

Transport by diffusion is the movement of solutes caused by a concentration gradient in soil solution. It is proportional to the effective diffusion coefficient D given by:

$$D = D_m + D_s \tag{15}$$

where D_m ($m^2\ s^{-1}$) is the molecular diffusion coefficient that, like D_s, is also a microscale process resulting from the average random motion of the molecules in the soil solution in response to the concentration gradient. It can be expressed by macroscopic variables as:

$$D_m = \xi D^0 \tag{16}$$

where ξ (–) is the tortuosity factor and D^0 ($m^2\ s^{-1}$) is the diffusion coefficient in water. Values of D^0 for ions or molecules can be easily measured and estimated by analytical equations for free water. Soil water is contained in a porous network, usually unsaturated, therefore diffusion will be different from that in free water. The tortuosity factor of Equation (16) can be calculated, for instance, by the empiric Millington-Quirk relation as:

$$\xi = \frac{\theta^{\frac{10}{3}}}{\theta_s^2} \tag{17}$$

The boundary conditions for solute transport are analogous to those presented for the case of water flow, but expressed in terms of concentrations instead of pressure heads. In microscopic models, commonly assumed boundary conditions are of zero, constant or variable solute flux at the root surface. The choice for one or another boundary condition depends on the way solute uptake by the plant is dealt with in the model (details in Section 3.5). For the outer boundary, a zero solute flux condition works well to simulate inter-root competition for solutes. A constant concentration – equal to the initial concentration – can be used in scenarios where the outer boundary is considered at a sufficient distance from the root surface so that competition between neighboring roots can be considered negligible. In macroscopic models, a sink-source term is added to Equation (12) to consider different inputs and outputs of solute in the system (*e.g.* plant uptake, mineralization, degradation, etc.), and the top and bottom boundaries are treated according to the scenario (similar to common practice when using the water flow equation).

3.5 Solute uptake by plant roots

The passage of water and solutes from soil to root, where plant physiological mechanisms may play a role, occurs at the root-soil interface. A correct mathematical treatment of this frontier is crucial for root water-solute uptake modeling. Different assumed conditions at this boundary originate distinct solutions for the convection-dispersion equation and, consequently, lead to distinct results. For a zero solute flux condition at the root surface, the solute will accumulate at the root surface due to convective flow. A consequent diffusion of solutes away from the root will result due to the formed concentration gradient and an equilibrium between convective and diffusive fluxes will establish. Differently, in the case of a constant or a variable solute uptake at the root surface, an accumulation of solute will result only if the uptake is less than the convective flow towards the root surface. If uptake exceeds convection, solute concentrations will decrease and eventually reach a zero (or limiting) concentration value. It is noticeable that the overall result of the model is highly dependent to the initial and boundary conditions, resulting in a wide range of possibilities.

Writing the convection-diffusion equation in its full form, by substituting Equation (13) in Equation (12) as

$$r\frac{\partial(\theta C)}{\partial t} = \frac{\partial}{\partial r}\left[D(\theta)\frac{\partial C}{\partial r} - qC\right] \tag{18}$$

and with a flux type boundary condition at r_0 and r_m of

$$-D(\theta)\frac{\partial C}{\partial r}\bigg|_{r=r_i} + qC = F\,, \quad t > 0,\ r_i = \{r_0, r_m\}\,, \tag{19}$$

all conditions of solute uptake rate can be defined by setting to F a specific uptake function. A zero solute uptake condition would be $F = 0$, a constant uptake condition would be $F = k$ and a concentration dependent uptake function would be $F = \alpha(C)k$, where k (mol m^{-2} s^{-1}) is a constant that represents the uptake rate and $\alpha(C)$ (–) a shape function for the uptake.

The rate of solute uptake by plant roots can be described by the MM equation, as seen in Chapter 2. The uptake shape function $\alpha(C)$ can be supposed to follow the concentration dependent MM kinetics, and considering k equal to I_m leads to:

$$\alpha(C) = \frac{C}{K_m + C} \Rightarrow F = \frac{C}{K_m + C}\, I_m \tag{20}$$

where I_m is the maximum uptake rate, C is the solute concentration in soil solution and K_m the Michaelis-Menten constant. I_m can be found experimentally and K_m is to be

calibrated as the concentration at which I_m assumes half of its value, being interpreted as the affinity of the plant for the solute.

The uptake rate according to Equation (20) is of asymptotic shape tending to saturation with increasing external concentration (Figure 1). It follows from the equation that, for very low concentration values ($C \ll K_m$), the uptake rate is proportional to concentration whereas, for $C \gg K_m$, the solute uptake rate is at its maximum and independent of concentration.

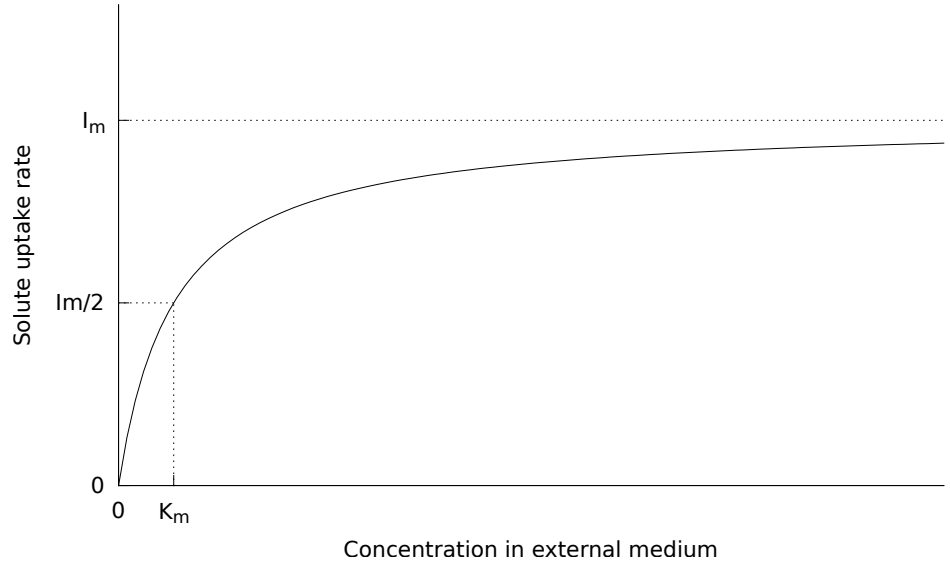

Figure 1 - Solute uptake rate as a function of external concentration according to the Michaelis-Menten kinetics (Equation (20))

4 METHODOLOGY

In this chapter, the model development is described. First, we show the mathematical equations that represent the transport of water and solutes and their uptake by the root (Section 4.1). The numerical development with the applied boundary conditions are show in Section 4.2. The numerical solutions for the zero (DE JONG VAN LIER; VAN DAM; METSELAAR, 2009) and constant uptake models – that were used in the comparison with the proposed model – are show in Sections 4.2.2 and 4.2.3 and a comparative analysis with the analytical model of Cushman (1979) is made in Section 4.3. Later, we present the description of the simulated scenarios (Section 4.4), a comparative analysis of the linear and non-linear approaches of the proposed model (Section 4.5) and its statistical difference (Section 4.6), and finally, the methodology used for the sensitivity analysis (Section 4.7).

4.1 General model description

The geometry of the soil-root system considers an uniformly distributed parallel cylindrical root of radius r_0 and length z. To each root, a concentric cylinder of radius r_m and length z can be assigned to represent its extraction volume (Figure 2).

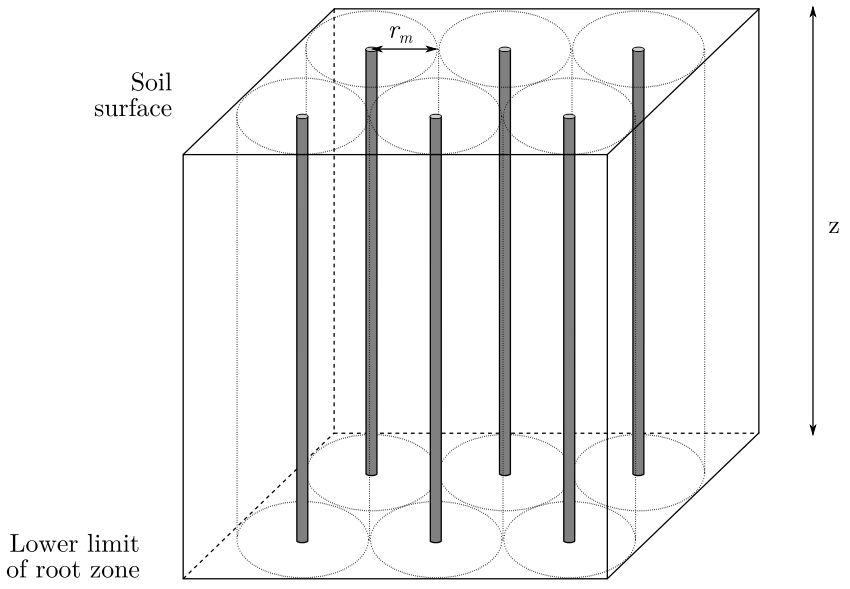

Figure 2 - Schematic representation of the spatial distribution of roots in the root zone

The discretization needed for the numerical solution was performed at the single root scale. As the extraction properties of the root are considered uniform along its length, and assuming no vertical differences in root density and fluxes, the cylinder can be represented by its cross-section, a circle. The area of this circle, representing the

extraction region, was subdivided into n circular segments of variable size Δr (m), small near the root and increasing with distance, according to the equation (DE JONG VAN LIER; VAN DAM; METSELAAR, 2009):

$$\Delta r = \Delta r_{min} + (\Delta r_{max} - \Delta r_{min}) \left(\frac{r - r_0}{r_m - r_0} \right)^S \tag{21}$$

where the subscripts in Δr indicate the minimum and maximum segment sizes defined by the user, and S gives the rate at which the segment size increases. The parameter r_0 (m) represents the root radius, and r_m (m) is the radius of the root extraction zone, equal to the half-distance between roots, which relates to the root density R (m m^{-3}) according to Equation (1). This variable size discretization has the advantage to result in smaller segments in regions that need more detail in the calculations (near the root soil interface) due to the greater variation of expected fluxes. Figure 3 shows a schematic representation of the discretization as projected by Equation (21).

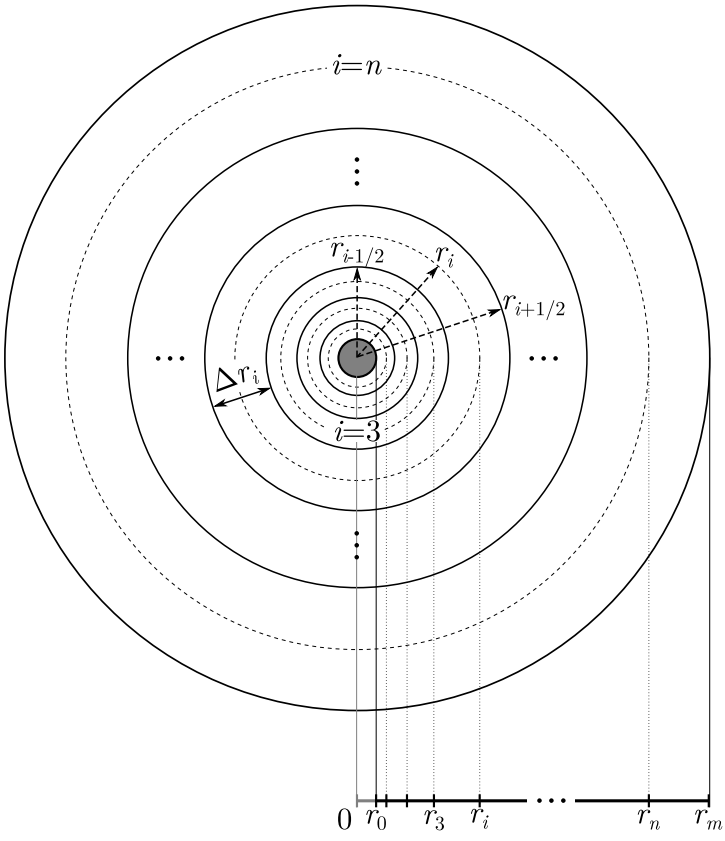

Figure 3 - Schematic representation of the discretized domain considered in the model. Δr is the variable segment size, increasing with the distance from the root surface (r_0) to the half-distance between roots (r_m), and n is the number of segments

A fully implicit numerical treatment was given to the water and solute balance equations (6) and (12). The Richards equation (6) for one-dimensional axis-symmetric

flow can be written as

$$\frac{\partial\theta}{\partial t} = \frac{\partial\theta}{\partial H}\frac{\partial H}{\partial t} = C_w(H)\frac{\partial H}{\partial t} = \frac{1}{r}\frac{\partial}{\partial r}\left(rK(h)\frac{\partial H}{\partial r}\right) \tag{22}$$

where the total hydraulic head (H) is the sum of pressure (h) and osmotic (h_π) heads and C_w (m^{-1}) is the differential water capacity $\dfrac{\partial H}{\partial\theta}$. Relations between K, θ and h are described by the Van Genuchten (1980) equation system (Equations (10) and (11)). Analogous to Van Dam and Feddes (2000), Equation (22) can be solved using an implicit scheme of finite differences with the Picard iterative process:

$$C_{wi}^{\,j+1,p-1}(H_i^{j+1,p} - H_i^{j+1,p-1}) + \theta_i^{j+1,p-1} - \theta_i^j = \frac{t^{j+1} - t^j}{r_i \Delta r_i} \times \left[r_{i-1/2} K_{i-1/2}^j \frac{H_{i-1}^{j+1,p} - H_i^{j+1,p}}{r_i - r_{i-1}} - r_{i+1/2} K_{i+1/2}^j \frac{H_i^{j+1,p} - H_{i+1}^{j+1,p}}{r_{i+1} - r_i} \right] \tag{23}$$

where i ($1 \leq i \leq n$) refers to the segment number, j is the time step and p the iteration level. The Picard's method is used to reduce inaccuracies in the implicit numerical solution for the h-based Equation (22) (CELIA; BOULOUTAS; ZARBA, 1990).

The solution for Equation (23) results in prediction of pressure head in soil as a function of time and distance from the root surface. The boundary conditions considered relate the flux density entering the root to the transpiration rate for the inner segment; and considers zero flux for the outer segment:

$$K(h)\frac{\partial h}{\partial r} = q_0 = \frac{T_p}{2\pi r_0 R z}\ , \qquad r = r_0 \tag{24}$$

$$K(h)\frac{\partial h}{\partial r} = q = 0\ , \qquad r = r_m \tag{25}$$

The computer algorithm that solves the Equation (23) and applies boundary conditions (24) and (25) can be found in Appendix B.

The convection-dispersion equation (12) for one-dimensional axis-symmetric flow can be written as

$$r\frac{\partial(\theta C)}{\partial t} = -\frac{\partial}{\partial r}\left(rqC\right) + \frac{\partial}{\partial r}\left(rD\frac{\partial C}{\partial r}\right). \tag{26}$$

with initial condition corresponding to constant solute concentration (C_{ini}) in all segments:

$$C = C_{ini}\ , \quad t = 0,\ r = r_i,\ 1 \leq i \leq n. \tag{27}$$

Both boundary conditions are of the flux type, according to Equation (19). From the assumed geometry (Figure 3) it follows that the boundary condition at the outer segment corresponds to zero solute flux (q_s):

$$D(\theta)\frac{\partial C}{\partial r} - qC = q_s = 0 \ , \qquad r = r_m. \tag{28}$$

The boundary condition for solute transport at the root surface represents the concentration dependent solute uptake, described by the MM equation (20), with the following assumptions:

1. Solute uptake by mass flow of water is only controlled by the transpiration flow, a convective flow that is considered to be passive;
2. Plant regulated active uptake corresponds to diffusion;
3. Plant demand is equal to the I_m parameter from the MM equation;
4. At a soil solution concentration value C_{lim}, the solute flux limits the uptake.

We assume that the plant demand for solute is constant in time. The uptake, however, can be higher or lower than the demand, depending on the concentration in the soil solution at the root surface (Figure 4). If the concentration is bellow a certain limiting value (C_{lim}), the uptake is limited by the solute flux, *i.e.* solute flux can not attend plant demand even with potential values of active uptake. Additionally, solute uptake by mass flow of water can be higher than the plant demand in situations of high transpiration rate and/or for high soil water content. In these cases, we assume that active uptake is zero and all uptake occurs by the passive process. A concentration C_2 (mol) for this situation is calculated. When the concentration is between C_{lim} and C_2, the uptake is equal to the plant demand as a result of the sum of active and passive contributions to the uptake. Assumption 1 states that passive uptake is not controlled by any physiological plant mechanisms and, in order to optimize the use of metabolic energy, active uptake is regulated in such way that it works as a complementary mechanism of extraction to achieve plant demand (Assumption 2). This results in a lower active uptake contribution than that of its potential value. However, the effect of the solute concentration inside the plant on solute uptake and plant demand is not considered in the model. Consequently, a scenario for which the demand is reduced due to an excess of solute concentration in the plant is not considered. This might, in certain situations, lead to an overestimated prediction of uptake.

A piecewise non-linear uptake function that considers these explicit boundary conditions was formulated as:

$$F = \begin{cases} \dfrac{I_m C_0}{K_m + C_0} + q_0 C_0, & \text{if } C_0 < C_{lim} \quad (29.1) \\ I_m, & \text{if } C_{lim} \leq C_0 \leq C_2 \quad (29.2) \\ q_0 C_0, & \text{if } C_0 > C_2 \quad (29.3) \end{cases}$$

with C_{lim} determined by the positive root of

$$C_{lim} = -\frac{K_m \pm \left({K_m}^2 + 4 I_m K_m / q_0\right)^{1/2}}{2}, \quad (30)$$

and C_2 by

$$C_2 = \frac{I_m}{q_0}. \quad (31)$$

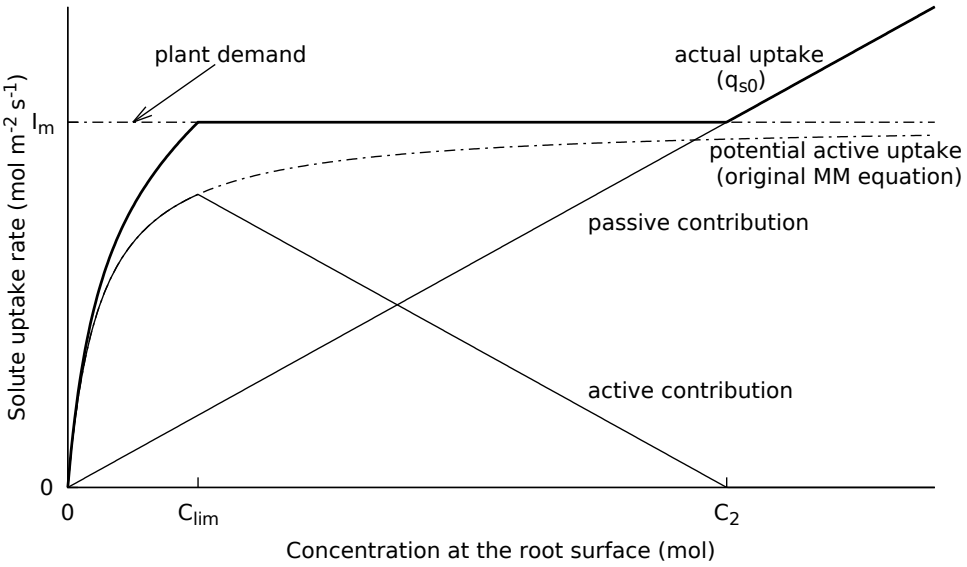

Figure 4 - Solute uptake piecewise equation (29) from MM equation (20) with boundary conditions. The bold line represents the actual uptake, thin lines represent active and passive contributions to the actual uptake, and dotted lines represent the plant demand and the potential active uptake

The non-linear part of the uptake function resides in Equation (29.1). As implicit numerical implementations of non-linear functions may result in solutions with stability issues, a linearization of Equation (29.1) was made, resulting in:

$$F = (\alpha + q_0)\, C_0, \quad \text{if } C_0 < C_{lim} \quad (32)$$

where α (m s^{-1}) and q_0 (m s^{-1}) are the active and passive contributions for the solute uptake slope ($\alpha + q_0$). This linearization is very similar to the one proposed by Tinker and Nye (2000), but does not consider the solute concentration inside the plant. The derivation of Equations (30) to (32) is shown in Appendix C.

Finally, the boundary condition at the inner segment refers to the concentration dependent solute flux at the root surface (F, mol m^{-2} d^{-1}) in agreement to Equation (29) and (32) for the non-linear and linear case, respectively. The uptake of each root equals $-F/R$ (mol d^{-1}, the negative sign indicating solute depletion), thus, the condition at the root surface is described by:

$$-D(\theta)\frac{\partial C}{\partial r} + q_0 C_0 = q_{s_0} = -\frac{F}{2\pi r_0 R z}\ , \qquad r = r_0 \tag{33}$$

4.2 Numerical implementations of the convection-dispersion equation

In this item, the numerical discretization and the applied boundary conditions are presented, together with the algorithm to find the solution of Equation (26) for both linear and non-linear boundary conditions at the root surface. The mass balance equations are considered to correspond to transient conditions with respect to water and solute.

As mentioned in the introduction of this chapter, besides the development of the proposed model (concentration dependent solute uptake), using the same discretization detailed in the previous section a numerical solution for a constant uptake model based on De Willigen and Van Noordwijk (1994) was developed. Additionally, we present the numerical solution for the zero uptake model (DE JONG VAN LIER; VAN DAM; METSELAAR, 2009), in which some modifications are proposed. In this text, zero uptake model will be abbreviated as ZU, constant uptake model as CU, linear concentration dependent model as LU and non-linear concentration dependent model as NLU.

In the numerical solutions, the combined water and solute movement is simulated iteratively. In a first step, the water movement towards the root is simulated, assuming salt concentrations from the previous time step. In a second step, the salt contents per segment are updated and new values for the osmotic head in all segments are calculated. The first step is then repeated with updated values for the osmotic heads. This process is repeated until the pressure head values and osmotic head values between iterations converge. Flowcharts containing the algorithm structure are shown in the Appendix D.

4.2.1 Concentration dependent uptake model (proposed model)

The implicit numerical discretization of Equation (26) yields:

$$\begin{aligned}\theta_i^{j+1}C_i^{j+1} - \theta_i^j C_i^j = \frac{\Delta t}{2r_i\Delta r_i}\times \\ \left\{\frac{r_{i-1/2}}{r_i - r_{i-1}}\left[q_{i-1/2}(C_{i-1}^{j+1}\Delta r_i + C_i^{j+1}\Delta r_{i-1}) - 2D_{i-1/2}^{j+1}(C_i^{j+1} - C_{i-1}^{j+1})\right] - \right. \\ \left.\frac{r_{i+1/2}}{r_{i+1} - r_i}\left[q_{i+1/2}(C_i^{j+1}\Delta r_{i+1} + C_{i+1}^{j+1}\Delta r_i) - 2D_{i+1/2}^{j+1}(C_{i+1}^{j+1} - C_i^{j+1})\right]\right\}\end{aligned} \tag{34}$$

Applying equation (34) to each segment, the concentrations for the next time step C_i^{j+1} (mol m^{-3}) are obtained by solving the following tridiagonal matrix:

$$\begin{bmatrix} b_1 & c_1 & & & & \\ a_2 & b_2 & c_2 & & & \\ & a_3 & b_3 & c_3 & & \\ & & \ddots & \ddots & \ddots & \\ & & & a_{n-1} & b_{n-1} & c_{n-1} \\ & & & & a_n & b_n \end{bmatrix} \begin{bmatrix} C_1^{j+1} \\ C_2^{j+1} \\ C_3^{j+1} \\ \vdots \\ C_{n-1}^{j+1} \\ C_n^{j+1} \end{bmatrix} = \begin{bmatrix} f_1 \\ f_2 \\ f_3 \\ \vdots \\ f_{n-1} \\ f_n \end{bmatrix} \tag{35}$$

with f_i(mol m^{-2}) defined as

$$f_i = r_i \theta_i^j C_i^j \tag{36}$$

and a_i (m), b_i (m) and c_i (m) defined for the respective segments as described in the following.

4.2.1.1 The intermediate nodes ($i = 2$ to $i = n - 1$)

Rearrangement of Equation (34) to (35) results in the coefficients:

$$a_i = -\frac{r_{i-1/2}(2D_{i-1/2}^{j+1} + q_{i-1/2}\Delta r_i)\Delta t}{2(r_i - r_{i-1})\Delta r_i} \tag{37}$$

$$b_i = r_i\theta_i^{j+1} + \frac{\Delta t}{2\Delta r_i}\left[\frac{r_{i-1/2}}{(r_i - r_{i-1})}(2D_{i-1/2}^{j+1} - q_{i-1/2}\Delta r_{i-1}) + \frac{r_{i+1/2}}{(r_{i+1} - r_i)}(2D_{i+1/2}^{j+1} + q_{i+1/2}\Delta r_{i+1})\right] \tag{38}$$

$$c_i = -\frac{r_{i+1/2}\Delta t}{2\Delta r_i(r_{i+1} - r_i)}(2D_{i+1/2}^{j+1} - q_{i+1/2}\Delta r_i) \tag{39}$$

4.2.1.2 The outer boundary ($i = n$)

Applying boundary condition of zero solute flux, the third and fourth terms from the right hand side of Equation (34) are equal to zero. Thus, the solute balance for this segment is written as:

$$\theta_n^{j+1}C_n^{j+1} - \theta_n^j C_n^j = \frac{\Delta t}{2r_n\Delta r_n} \times \left\{\frac{r_{n-1/2}}{r_n - r_{n-1}}\left[q_{n-1/2}(C_{n-1}^{j+1}\Delta r_n + C_n^{j+1}\Delta r_{n-1}) - 2D_{n-1/2}^{j+1}(C_n^{j+1} - C_{n-1}^{j+1})\right]\right\} \tag{40}$$

Rearrangement of Equation (40) to (35) results in the coefficients:

$$a_n = -\frac{r_{n-1/2}(2D_{n-1/2}^{j+1} + q_{n-1/2}\Delta r_n)\Delta t}{2(r_n - r_{n-1})\Delta r_n} \tag{41}$$

$$b_n = r_n\theta_n^{j+1} + \frac{\Delta t}{2\Delta r_n}\left[\frac{r_{n-1/2}}{(r_n - r_{n-1})}(2D_{n-1/2}^{j+1} + q_{n-1/2}\Delta r_{n-1})\right] \tag{42}$$

4.2.1.3 The inner boundary ($i = 1$)

a) **Linear concentration dependent model (LU)**

Applying boundary conditions of linear concentration dependent solute flux, the first and second terms of the right-hand side of Equation (34) are equal to $-\frac{\alpha + q_0}{2\pi r_o Rz} C_1^{j+1} \Delta r_1$ while $C < C_{lim}$ and $C > C_2$:

$$\theta_1^{j+1} C_1^{j+1} - \theta_1^j C_1^j = \frac{\Delta t}{2 r_1 \Delta r_1} \times \left\{ \frac{r_{1-1/2}}{r_1 - r_0} \left[-\frac{\alpha + q_0}{2\pi r_0 Rz} \right] C_1^{j+1} \Delta r_1 - \frac{r_{1+1/2}}{r_2 - r_1} \left[q_{1+1/2} (C_1^{j+1} \Delta r_2 + C_2^{j+1} \Delta r_1) - 2 D_{1+1/2}^{j+1} (C_2^{j+1} - C_1^{j+1}) \right] \right\} \quad (43)$$

When $C = 0$ the solute flux is set to zero and the equation is equal to Equation (50) (zero uptake). While $C_{lim} \leq C \leq C_2$, the solute flux density is constant and the equation is equal to Equation (54) (constant uptake).

The introduction of Equation (43) in the tridiagonal matrix (35) results in the following coefficients:

$$b_1 = r_1 \theta_1^{j+1} + \frac{\Delta t}{2 \Delta r_1} \left[\frac{r_{1+1/2}}{(r_2 - r_1)} (2 D_{1+1/2}^{j+1} + q_{i+1/2} \Delta r_2) + \frac{r_{1-1/2}}{(r_1 - r_0)} \frac{(\alpha + q_0)}{2\pi r_0 Rz} \Delta r_1 \right] \quad (44)$$

$$c_1 = -\frac{r_{1+1/2} \Delta t}{2 \Delta r_1 (r_2 - r_1)} (2 D_{1+1/2}^{j+1} - q_{1+1/2} \Delta r_1) \quad (45)$$

b) **Non-linear concentration dependent model (NLU)**

Applying boundary conditions of non-linear concentration dependent solute flux, the first and second term of the right-hand side of Equation (34) become $-\left(\frac{I_m}{2\pi r_0 Rz (K_m + C_1^{j+1})} + q_0 \right) C_1^{j+1} \Delta r_1$ for $C < C_{lim}$ and $C > C_2$:

$$\theta_1^{j+1} C_1^{j+1} - \theta_1^j C_1^j = \frac{\Delta t}{2 r_1 \Delta r_1} \times \left\{ \frac{r_{1-1/2}}{r_1 - r_0} \left[-\left(\frac{I_m}{2\pi r_0 Rz (K_m + C_1^{j+1})} + q_0 \right) \right] C_1^{j+1} \Delta r_1 - \frac{r_{1+1/2}}{r_2 - r_1} \left[q_{1+1/2} (C_1^{j+1} \Delta r_2 + C_2^{j+1} \Delta r_1) - 2 D_{1+1/2}^{j+1} (C_2^{j+1} - C_1^{j+1}) \right] \right\} \quad (46)$$

Rearrangement of Equation (46) to (35) results in the following coefficients:

$$b_1 = r_1 \theta_1^{j+1} + \frac{\Delta t}{2 \Delta r_1} \left[\frac{r_{1+1/2}}{(r_2 - r_1)} (2 D_{1+1/2}^{j+1} + q_{i+1/2} \Delta r_2) + \frac{r_{1-1/2}}{r_1 - r_0} \left(\frac{I_m}{2\pi r_0 Rz (K_m + C_1^{j+1})} + q_0 \right) \Delta r_1 \right] \quad (47)$$

$$c_1 = -\frac{r_{1+1/2} \Delta t}{2 \Delta r_1 (r_2 - r_1)} (2 D_{1+1/2}^{j+1} - q_{1+1/2} \Delta r_1) \quad (48)$$

The value of C_1^{j+1} in Equation (47) is found using the iterative Newton-Raphson method.

4.2.2 Zero uptake model (ZU)

The zero uptake solution is the original model presented by De Jong van Lier, Van Dam and Metselaar (2009). The numerical discretization is according to Equation (34) and the intermediate nodes are analogous to Equations (37) to (39). The only difference is the boundary at the root surface (Equation (33)), which is of zero solute flux:

$$q_{s0} = 0 \tag{49}$$

4.2.2.1 The inner boundary ($i = 1$)

Applying boundary condition of zero solute flux, the first and second term of the right-hand side of Equation (34) are equal to zero:

$$\theta_1^{j+1} C_1^{j+1} - \theta_1^j C_1^j = \frac{\Delta t}{2 r_1 \Delta r_1} \times \left\{ \frac{r_{1+1/2}}{r_2 - r_1} \left[-q_{1+1/2} (C_1^{j+1} \Delta r_2 + C_2^{j+1} \Delta r_1) + 2 D_{1+1/2}^{j+1} (C_2^{j+1} - C_1^{j+1}) \right] \right\} \tag{50}$$

Introduction of Equation (50) in the tridiagonal matrix (35) results in the following coefficients:

$$b_1 = r_1 \theta_1^{j+1} + \frac{\Delta t}{2 \Delta r_1} \left[\frac{r_{1+1/2}}{(r_2 - r_1)} (2 D_{1+1/2}^{j+1} + q_{1+1/2} \Delta r_2) \right] \tag{51}$$

$$c_1 = -\frac{r_{1+1/2} \Delta t}{2 \Delta r_1 (r_2 - r_1)} (2 D_{1+1/2}^{j+1} - q_{1+1/2} \Delta r_1) \tag{52}$$

4.2.3 Constant uptake model (CU)

The constant uptake solution is based on the model proposed by De Willigen and Van Noordwijk (1994). The numerical discretization takes into consideration Equation (34), whereas the intermediate nodes are analogous to Equations (37) to (39). The boundary condition at the root surface (Equation (33)) corresponds to constant solute flux:

$$q_{s0} = -\frac{I_m}{2 \pi r_0 R z}. \tag{53}$$

4.2.3.1 The inner boundary ($i = 1$)

Applying boundary conditions of constant solute flux, the first and second term of the right-hand side of Equation (34) become $-\frac{I_m}{2\pi r_0 Rz}\Delta r_1$ for $C > 0$:

$$\begin{aligned}\theta_1^{j+1}C_1^{j+1} - \theta_1^j C_1^j = \frac{\Delta t}{2r_1\Delta r_1}\times \\ \left\{\frac{r_{1-1/2}}{r_1 - r_0}\left(-\frac{I_m}{2\pi r_0 Rz}\right)\Delta r_1 - \right. \\ \left.\frac{r_{1+1/2}}{r_2 - r_1}\left[q_{1+1/2}(C_1^{j+1}\Delta r_2 + C_2^{j+1}\Delta r_1) - 2D_{1+1/2}^{j+1}(C_2^{j+1} - C_1^{j+1})\right]\right\}\end{aligned} \tag{54}$$

When $C = 0$ the solute flux is set to zero and equation (54) reduces to Equation (50).

Introduction of Equation (54) in the tridiagonal matrix (35) results in the following coefficients:

$$b_1 = r_1\theta_1^{j+1} + \frac{\Delta t}{2\Delta r_1}\left[\frac{r_{1+1/2}}{(r_2 - r_1)}(2D_{1+1/2}^{j+1} + q_{1+1/2}\Delta r_2)\right] \tag{55}$$

$$c_1 = -\frac{r_{1+1/2}\Delta t}{2\Delta r_1(r_2 - r_1)}(2D_{1+1/2}^{j+1} - q_{1+1/2}\Delta r_1) \tag{56}$$

$$f_1 = r_1\theta_1^j C_1^j - \frac{r_{1-1/2}}{r_1 - r_0}I_m\frac{\Delta t}{4\pi r_0 Rz} \tag{57}$$

4.3 Comparison to other solute uptake models

The model developed in this thesis is compared to (1) the ZU model (Section 4.2.2) of De Jong van Lier, Van Dam and Metselaar (2009); (2) the CU model (Section 4.2.3) based on the analytical model of De Willigen and Van Noordwijk (1994); and (3) the analytical model of Cushman (1979), described in the following.

A computational implementation of the analytical model of Cushman (1979) was performed to confront it with the non-linear numerical solution (NLU). This particular analytical model also uses the MM equation as boundary condition for solute uptake at the root surface. The equation by Cushman (1979) is:

$$\Theta(\mu, \eta) = \sum_{n=0}^{\infty} A_n \mu^v \beta_v(\mu, \tau, \alpha_n)\exp(-\alpha_n^2\eta) + 1 \tag{58}$$

where

$$\begin{aligned}\beta_v(\mu, \tau, \alpha_n) = [\alpha_n a Y_{v-1}(a\alpha_n) - 2v(1-\tau)Y_v(\alpha_n)]\, J_v(\alpha_n\mu) \\ - [\alpha_n a J_{v-1}(a\alpha_n) - 2v(1-\tau)J_v(\alpha_n)]\, Y_v(\alpha_n\mu),\end{aligned} \tag{59}$$

the α_n are roots of

$$[\alpha a J_{v-1}(\alpha a) - 2v J_v(\alpha a)][\alpha Y_{v-1}(\alpha) - 2v(1-\tau)Y_v(\alpha)] + \tag{60}$$
$$[2v Y_v(\alpha a) - \alpha a Y_{v-1}(\alpha a)][\alpha J_{v-1}(\alpha) - 2v(1-\tau)J_v(\alpha)] = 0,$$

and the A_n are given by

$$A_n = -\frac{\int_1^a \mu^{1-v}\beta_v(\mu,\tau,\alpha_n)d\mu}{\int_1^a \mu {\beta_v}^2(\mu,\tau,\alpha_n)d\mu}. \tag{61}$$

This analytical solution corresponds to a linear boundary condition. The simplification was based on the assumption that the solute concentration is initially low, making the non-linear MM equation to become linear:

$$\frac{kC}{1+kCJ_{max}} \approx kC \tag{62}$$

and the boundary condition to become

$$D\frac{\partial C}{\partial r} + q_0 C = kC. \tag{63}$$

The non-dimensional variables η, μ, τ, Θ, v and a account for time, distance, root ability to absorb solute by convective flux, solute concentration in soil solution, ratio of convective to diffusive flux and outer influence of the root, respectively, and they are related to the dimensional variables as follows:

$$\eta = t\frac{D}{{r_0}^2} \tag{64}$$
$$\mu = \frac{r}{r_0} \tag{65}$$
$$\Theta(\mu,\eta) = \frac{C_{ini} - C_s(r,t)}{C_{ini}} \tag{66}$$
$$v = -\frac{r_0 q_0}{2Db} \tag{67}$$
$$\tau = \frac{k}{q_0} \tag{68}$$
$$a = r_m/r_0 \tag{69}$$

where t (T) is time, D (L^2 T^{-1}) is the diffusion coefficient, r_0 (L) is the root radius, r (L) is the distance from root center, C_{ini} (M L^{-3}) is the initial solute concentration, C_s (M L^{-3}) is the solute concentration in bulk soil, q_0 (L T^{-1}) is the flux of water, b ($\frac{dC_s}{dC}$) is the differential buffer power, C (M L^{-3}) is the solute concentration in soil solution, and k (L T^{-1}) is the root absorbing power (equal to K_m in the nomenclature of this thesis). A more detailed description of the model and its variables and boundary conditions is found in Cushman (1979) and in Nye and Marriott (1969).

4.4 Simulation scenarios

The simulations were performed using the hydraulic parameters from the Dutch Staring series (WÖSTEN et al., 2001) for three different soils types, as listed in Table 1. The general system parameters for the different scenarios are listed in Table 2 and values for the Michaelis-Menten (MM) parameters in Table 3. Values of root length density, initial solute concentration, relative transpiration, soil type, and ion species were chosen at several values, composing eight distinct scenarios as listed in Table 4. Scenario 1 was considered as default, the other scenarios derive from scenario 1 by changing only one input parameter. In this way, the effect of variation in soil hydraulic properties is exemplified by scenarios 1, 6 and 7; root length density by scenarios 1, 4 and 5; initial solute concentration by scenarios 1 and 3; and potential transpiration by scenarios 1 and 2.

Table 1 - Soil hydraulic parameters used in simulations

Staring soil ID	**Textural class**	**Reference in this thesis**	θ_r $m^3\,m^{-3}$	θ_s $m^3\,m^{-3}$	α m^{-1}	**l** –	**n** –	K_s $m\,d^{-1}$
B3	Loamy sand	Sand	0.02	0.46	1.44	-0.215	1.534	0.1542
B11	Heavy clay	Clay	0.01	0.59	1.95	-5.901	1.109	0.0453
B13	Sandy loam	Loam	0.01	0.42	0.84	-1.497	1.441	0.1298

Source: Wösten et al. (2001)

Table 2 - System parameters used in simulations scenarios

Description	**Symbol**	**Scenario description**	**Value**	**Unit**
Root radius	r_0		0.5	mm
Root depth	z		20	cm
Limiting root potential	H_{lim}		-150	m
Root density	R	Low root density Medium root density High root densit	0.01 0.1 1	cm cm^{-3}
Half distance between roots	r_m	Low root density Medium root density High root densit	56.5 17.8 5.65	mm
Potential transpiration rate	T_p	Low High	3 6	mm d^{-1}
Initial solute concentration in bulk soil	C_{ini}	Low High	1 10	mol m^{-3}
Initial pressure head	h_{ini}		-1	m
Diffusion coefficient in water	$D_{m,w}$		$1.98 \cdot 10^{-9}$	$m^2\ s^{-1}$
Dispersivity	τ		0.0005	m
Soil type		Sand Clay Loam	Table 1	

Source: De Jong van Lier, Van Dam and Metselaar (2009)

Table 3 - Michaelis-Menten parameters for some solutes

Solute	I_m mol m^{-2} s^{-1}	K_m mol m^{-3}
NO_3^-	10^{-5}	0.05
K^+	$2 \cdot 10^{-6}$	0.025
$H_2PO_4^-$	10^{-6}	0.005
Cd^{2+}	10^{-6}	1

Source: Roose and Kirk (2009)

Table 4 - Simulation scenarios*

Scenario	**R**	C_{ini}	T_p	**Soil**	**Ion**
1	M	H	H	Loam	K^+
2	M	H	L	Loam	K^+
3	M	L	H	Loam	K^+
4	H	H	H	Loam	K^+
5	L	H	H	Loam	K^+
6	M	H	H	Sand	K^+
7	M	H	H	Clay	K^+
8	M	H	H	Loam	NO_3^-

*H - high; M - medium; L - low; R - root length density; C_{ini} - initial concentration; T_p - potential transpiration

The default values of Δr_{min}, Δr_{max} and S in Equation (21) were 10^{-5} m, 5 10^{-4} m and 0.5, resulting in 22, 68 and 213 segments for the high, medium and low root density simulations, respectively. To guarantee complete convergence for the non-linear model, a time step of 0.01 s was used when $C_0 < C_{lim}$. Parameters h_{ini} and C_{ini} were chosen such that the plant is in a no stress condition ($T_r = 1$). All simulation scenarios ended when $T_r \leq 0.001$, at that point considering water uptake to be negligible.

4.5 Analysis of linear and non-linear approaches

To analyze the differences between the two proposed models (linear and non-linear solutions), the relative differences in the predicted concentrations (δ_C) and accumulated uptake (δ_{Ac}), for both models, were calculated as follows:

$$\delta_C = \frac{\sum_{x=1}^{x_{end}} CL_x - CNL_x}{\sum_{x=1}^{x_{end}} CL_x} \tag{70}$$

$$\delta_{Ac} = \frac{\sum_{t=1}^{t_{end}} AcL_t - AcNL_t}{\sum_{t=1}^{t_{end}} AcL_t} \tag{71}$$

where CL_x and CNL_x, are the solute concentration in soil water, and AcL_t and $AcNL_t$ the accumulated uptake, for LU and NLU, respectively. x can be the time (t) or the distance from the axial center (r). The relative difference between three outputs was computed: two relative to time – concentration at the root surface $C_0(t)$ and accumulated solute uptake $Ac(t)$ – and one relative to radial distance – concentration $C(r)$.

NLU solution uses the non-linear MM equation (29) and, due to an additional iterative process in the numerical implementation, more time is needed to compute the results when compared with the linear solution LU. It is also susceptible to numerical stability issues, depending on selected time and space steps. On the other hand, LU is a simplified version of the MM equation in a way that the solute uptake rate for $C_0 < C_{lim}$ is always smaller than that of the original non-linear equation. It has no stability problems and needs less computational time because it is less sensitive to space and time steps. In a first analysis, the objective was to check if the difference in the results generated by the linearization of the MM equation is sufficiently large to be properly analyzed. To do so, four different scenarios were chosen (scenarios 1 to 4 as listed in Table 4).

4.6 Statistical difference

The Mann–Whitney U test (MCKNIGHT; NAJAB, 2010) was performed with three datasets for the two models and for each scenario: (1) concentration over time – $C_0(t)$; (2) accumulated uptake over time – $Ac(t)$; (3) concentration over radial distance – $C(r)$). This test was chosen because the frequency distributions for both datasets are not normal, the pairs (datasets for LU and NLU) are distinct and do not affect each other. This test can distinguish whether each pair is identical or not without assuming them to follow the normal distribution (nonparametric test). The null hypothesis (H_0) is that both groups do not differ from each other and the alternate hypothesis (H_1) is that groups are different.

The interpretation of test results allows to decide in which cases a particular model should be used (in case they are different) or if both models are equally useful (in case they present no statistical difference).

4.7 Sensitivity analysis

The relative partial sensitivity η (DE JONG VAN LIER; WENDROTH; VAN DAM, 2015) of model predictions Y as a function of the respective parameter value P was calculated as

$$\eta = \frac{dY/Y}{dP/P} \tag{72}$$

where P is the default value of the parameter, dP is the in(de)crement applied to P, Y is the output of a selected predicted variable and dY is the variation over Y when applied the new parameter value $P \pm dP$.

To determine the sensitivity of the model to an input parameter, the magnitude of its derivative in respect of the model result is calculated. If this derivative is close to zero, the model has a low sensitivity to the respective parameter. The higher the derivative, the higher is the sensitivity and, therefore, the higher is the precision required when determining that parameter. By making a relative analysis like in Equation (72), the sensitivity for distinct parameters can be compared.

To determine the sensitivity, a dP/P of 0.01 (1%) was used for the following selected parameters: a) MM parameters I_m, K_m; and b) soil hydraulic parameters α, n, λ, K_s, θ_r and θ_s. The analyzed predicted variables (Y) were: time to completion of simulation t_{end}, osmotic head at completion of simulation h_π, pressure head at completion of simulation h, average osmotic head in the soil profile at completion of simulation $\overline{h_\pi}$, average pressure head in soil profile at completion of simulation $\overline{h}$ and accumulated uptake at completion of simulation Ac.

5 RESULTS AND DISCUSSION

5.1 Linear (LU) versus non-linear (NLU) solutions

According to Equations (29) and (32), the difference between LU and NLU will only shows up when the solute concentration at the root surface is lower than C_{lim}, resulting in a different boundary condition for each model. This condition ($C_0 < C_{lim}$) will be referred to as 'limiting concentration condition', abbreviated as LCC. In this section, we will analyze the predictions of LU and NLU and if these predictions are significantly different, in which case one model would be preferred over the other.

The differences between the two models were not significant when the complete time series is considered in calculations (from the initial to the final time step). This is because the low value of C_{lim} causes LCC to occur only during a short fraction of time. In scenario 1, for instance, the duration of occurrence of LCC is about 3% of the total simulation time. Moreover, due to the low value of C_{lim}, the LCC always coincides to very low solute uptake rates in all simulation scenarios. Therefore, the difference in predictions for the two models are of minor relevance at this time scale. Figure 5 gives an example of this: the cumulated amount of solute extracted by the roots until the completion of the simulation is nearly the same for both models. In addition, the LCC occurs at values of relative transpiration (T_r, the ratio between actual and potential transpiration) around 0.03 or less – a condition at which the plant is at high (combined water and osmotic) stress levels – and close to the completion of simulation (when $Tr \leq 0.001$).

Figure 6 shows that abrupt transpiration reductions may occur for both models as a result from two distinct processes. The first one (indicated by #1 in Figure 6) is caused by the combined water and osmotic stress resulted from the decreasing water flux towards the root when the total hydraulic head H reaches the limiting value H_{lim} of -150 m (similarly observed by De Jong van Lier, Van Dam and Metselaar (2009)). The second reduction (#2 in Figure 6) is due to the decrease of the solute uptake rate that results from the change in the boundary condition at the onset of LCC, causing a decreasing (more negative) value for the osmotic head h_π. As H at the root surface is not allowed to reduce below H_{lim}, the model predicts lower (less negative) h values resulting in smaller water flux rates at the root surface (q_0), reflecting in a lowered T_r. Therefore, this second reduction depends on the value of q_0, which directly affects the C_{lim} value (Equation (30)), and it abruptly reduces the relative transpiration due to the combined water and osmotic stress. This limiting concentration, here only numerically computed, may be controlled

by physical or physiologic processes and needs to be investigated. The NLU causes a smoother T_r reduction over time in the second reduction (Figure 6), apparently more appropriate for a natural phenomenon.

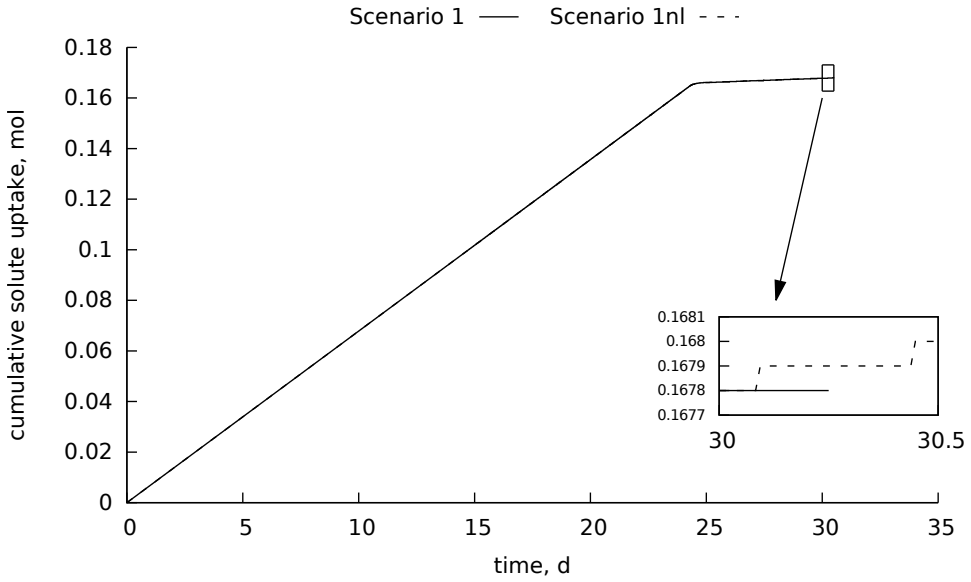

Figure 5 - Cumulative solute uptake as a function of time for scenario 1, predicted be the linear (solid line) and the non-linear (dashed line) model

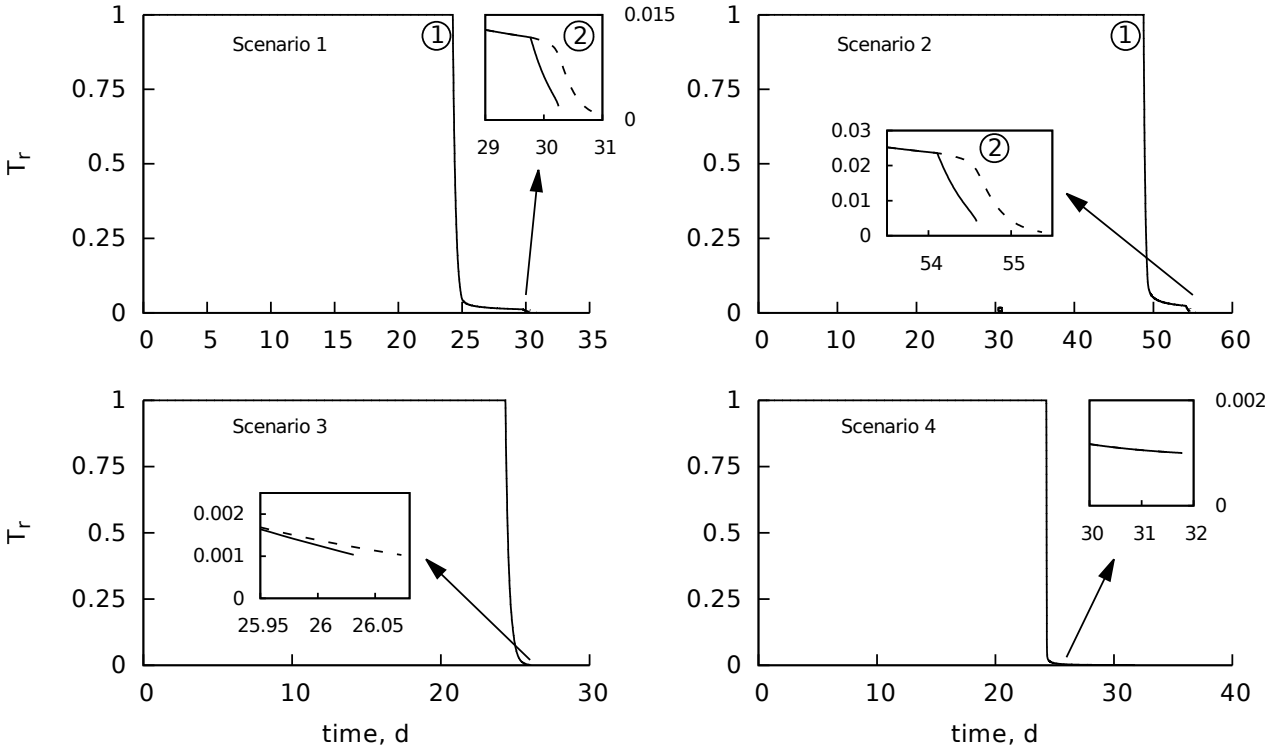

Figure 6 - Relative transpiration as a function of time for scenarios 1 to 4, predicted by the linear (solid line) and the non-linear (dashed line) model. Numbers inside circles represent the first and the second T_r reduction

Differences between both model predictions can become more significant by increasing the value of C_{lim}, causing LCC to be reached in an earlier phase and therefore

representing a larger fraction of total time. C_{lim} is not an input parameter, but it can be increased for the same ion species by decreasing the water flux at the root surface (Figure 7), which may be established by reducing the initial water content, for example. A change in ion or plant species would also modify the I_m and K_m parameters and, therefore, the relation between C_{lim} and q_0. Due to the nature of Equation (30), the C_{lim} value asymptotically increases, tending to infinity with decreasing q_0. Therefore, a value of C_{lim} resulting in a more significant difference between LU and NLU will occur for q_0 (and relative transpiration) close to zero. Considering the dependence between C_{lim} and q_0, no combination of initial parameters was encountered leading to a significant increase of the difference between LU and NLU. On the other hand, if only the predictions during the occurrence of LCC are computed, differences become significant.

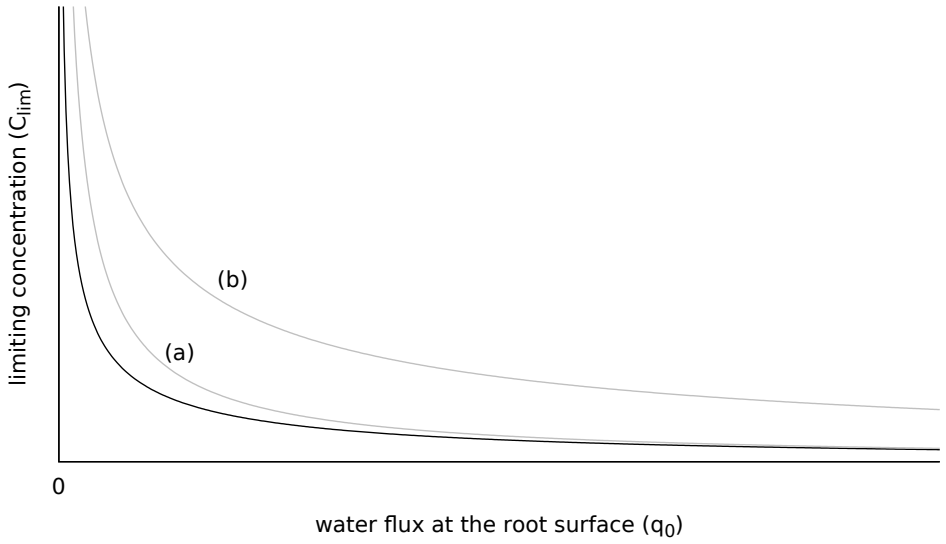

Figure 7 - Representative curve of the limiting concentration as a function of water flux, according to Equation (30) (black line). Grey lines represent equal increases in (a) K_m and (b) I_m parameters

Table 5 shows the relative difference between the model predictions for concentration at the root surface as function of time ($C_0(t)$), considering only the LCC phase (starting at LCC onset), and for the solute concentration as a function of distance from the axial center ($C(r)$) at completion of the simulation. The Mann-Whitney U test showed a significant difference for $C_0(t)$ but not for $C(r)$. The absolute difference (δ) between LU and NLU increases with time (Figure 8). Concentration as a function of radial distance (Figure 9) shows a different behavior, as solutes in each segment are replenished by the neighboring segment, making the difference smaller with increasing distance. Scenario 4

Table 5 - Relative difference between LU and NLU for the selected model outputs, for the condition $C_0 < C_{lim}$. The sign * represents a significant difference with confidence interval of 95% by the Mann-Whitney U test

Scenario	$C_0(t)$ mol m^{-3}	$C(r)$ mol m^{-3}
1	42.964*	2.370
2	43.497*	2.484
3	89.753*	2.342
4	0	0

did not reach the LCC within the simulation period and Table 5 shows the differences only to occur when starting from a $C_0 < C_{lim}$ condition.

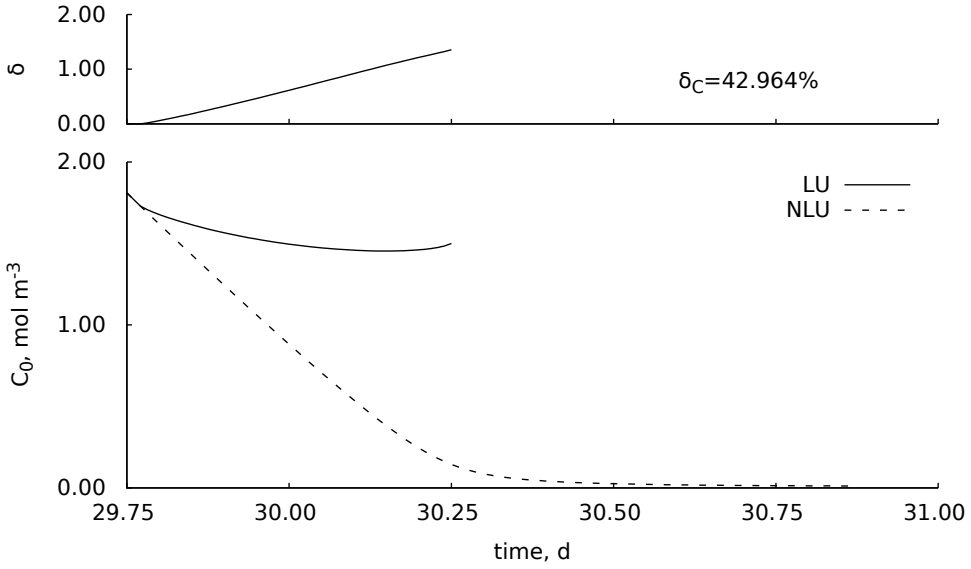

Figure 8 - (bottom) Solute concentration at the root surface as a function of time for scenario 1 during LCC occurrence predicted by the linear (solid line) and non-linear (dashed line) model; (top) absolute difference (δ) between the two models and its relative difference (δ_c) value according to Equation (70)

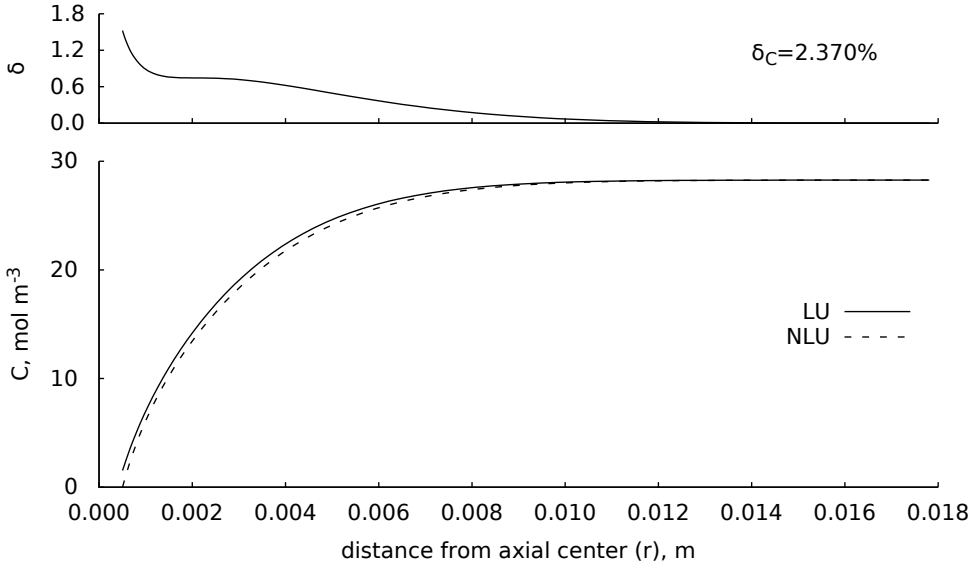

Figure 9 - (bottom) Solute concentration as a function of distance from axial center for scenario 1 during LCC occurrence predicted by the linear (solid line) and non-linear (dashed line) model; (top) absolute difference (δ) between the two models and its relative difference (δ_c) value according to Equation (70)

These results indicate that the difference in predictions of both models are relevant only during LCC, in other words, the difference between linear and non-linear boundary conditions is significant during LCC for root surface concentration predictions as a function of time ($C_0(t)$). Regarding the prediction of concentration as a function of distance from axial center ($C(r)$), there is no significant difference between both models. Therefore, predictions that result from the entire simulation period, like accumulated uptake, or for concentration as a function of the radial distance, show very small differences only and both models perform equally. In these cases, LU may be preferred since it allows larger time steps reducing simulation computing time. On the other hand, by considering that the metabolic response of the plant for different levels of concentration at the root surface is immediate – only a slightly change in C_0 causes a instantaneous plant reaction – or in situations where the value of C_0 during LCC is important, NLU could be preferred as the mechanistically most correct model. In this thesis we chose to use NLU since the values of C_0 affect the active and passive contributions to the solute uptake, which will be analyzed in Section 5.3.

It is important to mention some issues with stabilization in the numerical solution of NLU. The introduction of the non-linear uptake rate boundary condition – Equation (29) – may cause numerical instability at the initial times if time and space steps are not chosen carefully. Many different time and space step combinations were tested for each scenario, until satisfying results were obtained. We found that, as a rule, a small time step of 0.01 s can be used when the default values of space parameters Δr_{min} and Δr_{max} (Section 4.4) are used. When a smaller space step is necessary, smaller values of Δt are required. The Von Neumann stability analysis (VON NEUMANN; RICHTMYER, 1950) shows that, for a hydrodynamic equation, a good criterion to choose the time step is $\Delta t \leq \frac{\Delta r^2}{2D}$. However, to show stable solutions, the model required smaller values of Δt than the ones suggested by the Von Neumann stability criteria. The reason may reside in the fact that Von Neumann's criterion assumes constant values of D and Δr. In the proposed model, the space step increases with increasing distance in a way that a variable space discretization is formed rather than a fixed size set of space steps. For a medium root length density scenario, for example, Δr values ranged from $0.005 \cdot 10^{-4}$ to $2.8 \cdot 10^{-4}$ m when using the default values of space parameters. Similarly, the diffusion coefficient

D is not constant as it is computed for each space step according to the water flux and the water content of the respective segment.

Roose and Kirk (2009) stated that, for numerical solutions of convection-dispersion equation, the convective part might use an explicit scheme because convection, unlike diffusion, occurs only in one direction thus the solution at the following time step depends only on the values within the domain of influence of the previous time step. This imposes bounds on time and space steps, with a condition of stability given by $\frac{r_0 q_0 \Delta t}{D} < \Delta r$. The proposed model uses a fully implicit numerical scheme that may be another cause of instability. A stability analysis that considers the use of an implicit scheme for the numerical solution together with variable space steps and diffusion coefficients is a challenge for this type of modelling, aiming to reach more efficient and reliable calculations. As a result of the selected time step value (0.01 s), the time to complete a simulation run ranged from 40 minutes to 1.5 days, in our simulation scenarios, using a state-of-the-art computer with a 3.2 GHz processor (theoretical performance: 12.8 GFLOPS – billion floating-point operations per second). Decreasing Δt leads to an increase of the number of calculations and requires more computing time.

5.2 Solute uptake models comparison

In this section, the predictions of the ZU, the CU and the analytical model are shown in comparison to the non-linear model (NLU), for Scenario 1.

5.2.1 Analytical model

The proposed non-linear numerical model is compared to the analytical model of Cushman (1979), in Figure 10, with input parameters of scenario 1. The boundary conditions of the analytical model constrain it to a constant water uptake and dispersion coefficient (steady state condition). Therefore, average values for the simulated water flux and dispersion coefficient of scenario 1 were calculated to serve as inputs in the analytical model. The simulated time to evaluate the concentration profile in the analytical model was the same of the numerical model for scenario 1 ($t_{end} = 30$ days).

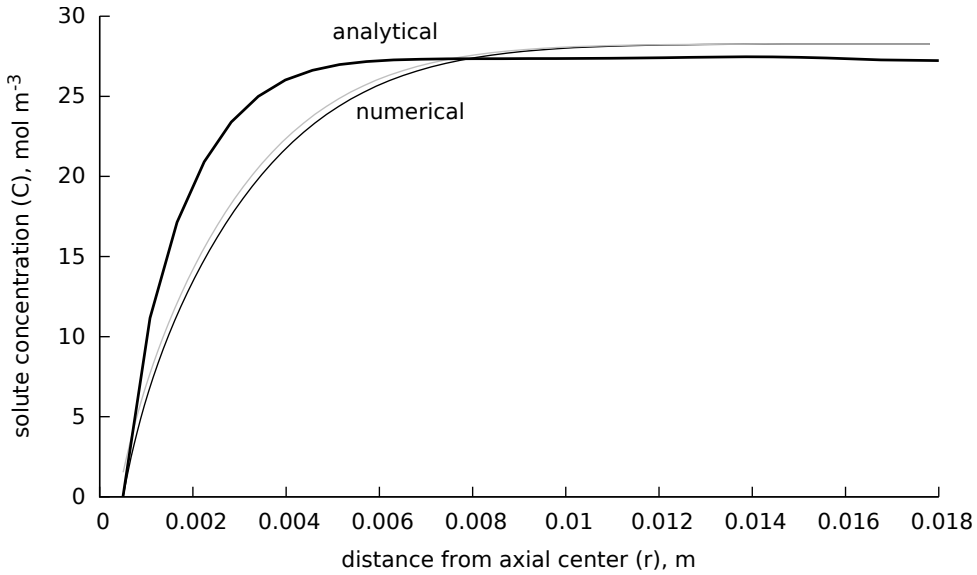

Figure 10 - Solute concentration profile predicted by the analytical model of Cushman (1979) (bold line) and by the non-linear (thin black line) and linear (thin grey line) numerical models, with parameters of scenario 1, at time $t = 30$ days

The differences between the two models is mostly due to the consideration of steady state condition in respect to water flow in the analytical model as opposed to the proposed numerical model that deals with transient water and solute fluxes. Discussion in Section 5.1 makes clear that there is no significant difference between the results of concentration profile of LU and NLU models. Nevertheless, Figure 10 also shows the concentration profile for the LU model, considering that the analytical model has a linear solute uptake rate as the boundary condition at the root surface. With the assumption of linearity (Equation (62)) in the analytical solution, the boundary condition equation has 1 (k) instead of 2 (J_{max} and k) parameters, which can overestimate the uptake at high concentrations.

Despite the differences in the assumptions and input values of each model, the numerical model shows good agreement with the analytical solution by Cushman (1979), which is plausible as they are simulating the same phenomenon over an almost identical scenario. The proposed numerical model can then be used as an alternative to the analytical model, with the advantage of simulate transient water and solute fluxes, giving the possibility to predict the solute uptake of a wider range of scenarios.

5.2.2 Numerical models

According to the piecewise Equation (29), the solute uptake rate occurs in three phases. They will be abbreviated LUP – linear uptake phase when $C_0 > C_2$, CUP –

constant uptake phase when $C_{lim} < C_0 < C_2$, and NUP – non-linear uptake phase when $C_0 < C_{lim}$, as shown in Figure 11.

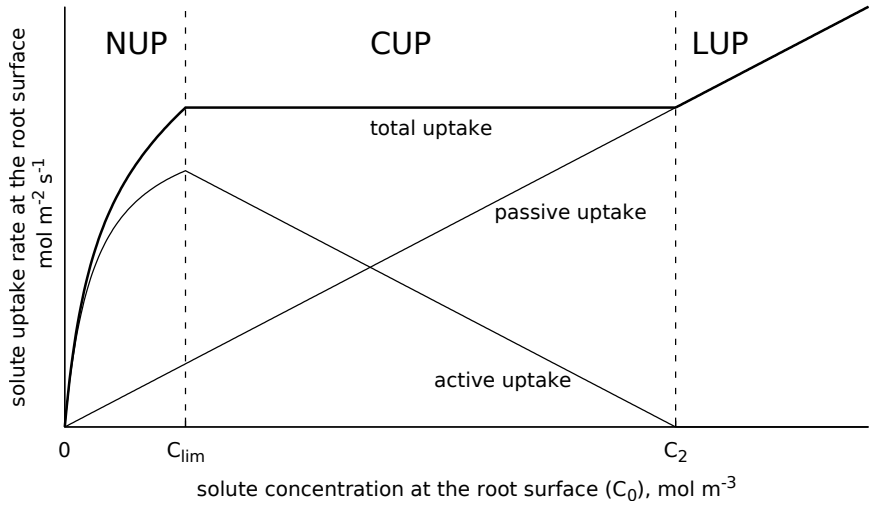

Figure 11 - Schematic representation of the phases LUP ($C_0 > C_2$), CUP ($C_{lim} < C_0 < C_2$) and NUP ($C_0 < C_{lim}$)

Predictions of solute concentration at the root surface as a function of time for three different models ZU, CU and NLU are shown in Figure 12. According to ZU, solutes are transported to the roots by convection, causing an accumulation of solutes at the root surface. As water flux towards the root starts to decrease, salt is transported slower and carried away from the roots by diffusion. CU results in a similar prediction with a slightly lower C_0 value because the convective solute flux towards the root is much higher than the constant uptake rate I_m, making solutes to accumulate at the root surface. With higher I_m values, less solute will be predicted to accumulate at the root surface by the CU model and CU and NLU predictions will become more similar (demonstrated in Figure 12 by the grey line).

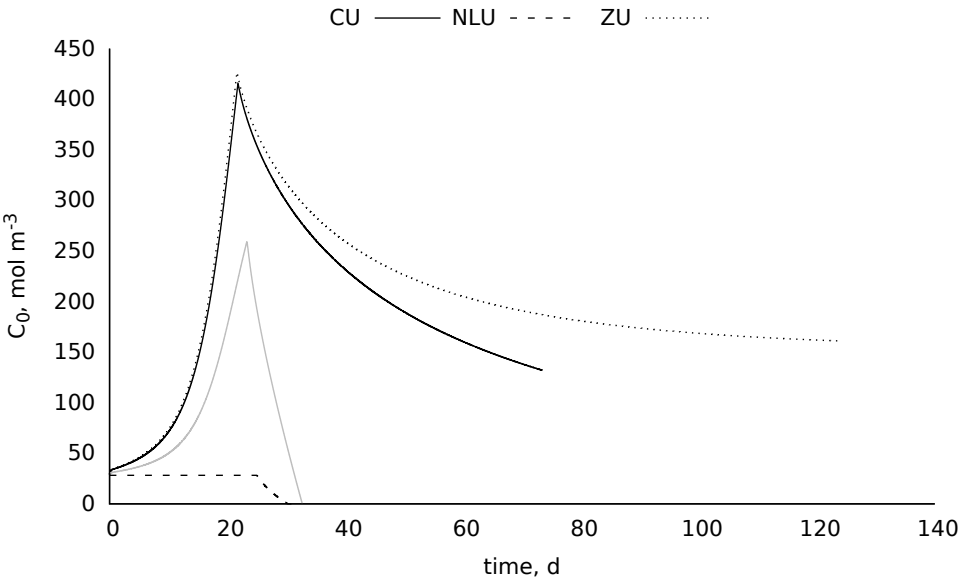

Figure 12 - Soil solution concentration at the root surface as a function of time predicted by the constant (CU), zero (ZU) and non-linear (NLU) uptake models for scenario 1. Gray line is CU with an arbitrary chosen 10 times higher value for the constant of solute uptake rate ($I_m = 2 \cdot 10^{-5}$ mol cm^{-2} s^{-1})

For ZU and CU, C_0 starts to diminish (corresponding to less negative values of h_π) as soon as $T_r < 1$, because H at the root surface reached the limiting value of -150 m (Figure 13). In CU, as the solute uptake is constant and does not depend on the solute concentration, the solute transport by convection becomes less important than the movement by diffusion as the water flux towards the root diminishes. Thus, the solute depletion at the root surface is due both to the uptake and to the diffusive transport away from the roots. For the case of NLU (Figure 14), an accumulation phase does not develop due to the high solute uptake rate in LUP (Figure 15), resulting from the model assumption that all solute carried by mass flow of water (convective transport) that reaches the root surface is taken up. Moreover, the higher uptake of NLU causes lower values of osmotic head (h_π) and results in a prediction of a longer period of potential transpiration ($T_r = 1$). For the case of CU and ZU, reduction of T_r starts around day 21 whereas for NLU it onsets on about day 24.

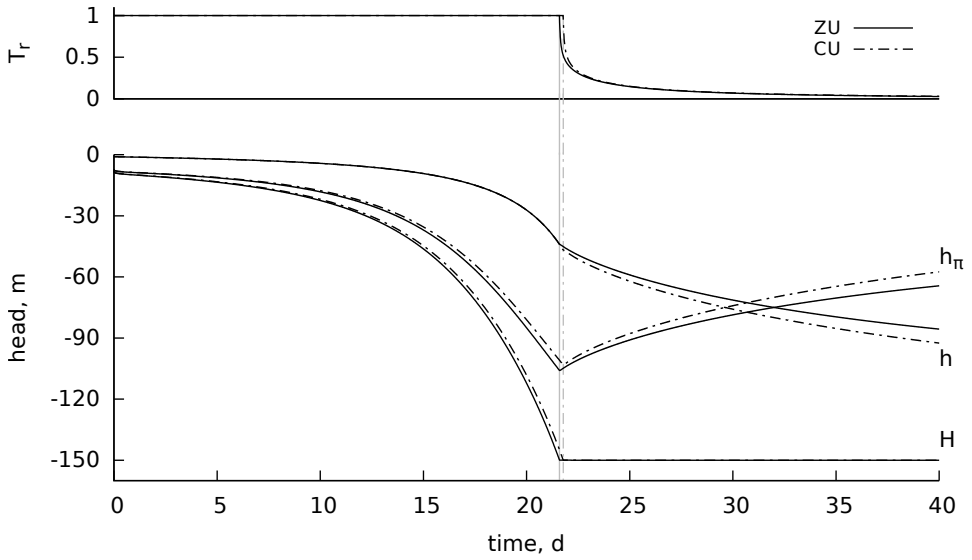

Figure 13 - Pressure (h), osmotic (h_π) and total hydraulic (H) heads at the root surface as a function of time predicted by the constant (CU) and the zero (ZU) uptake models, for scenario 1

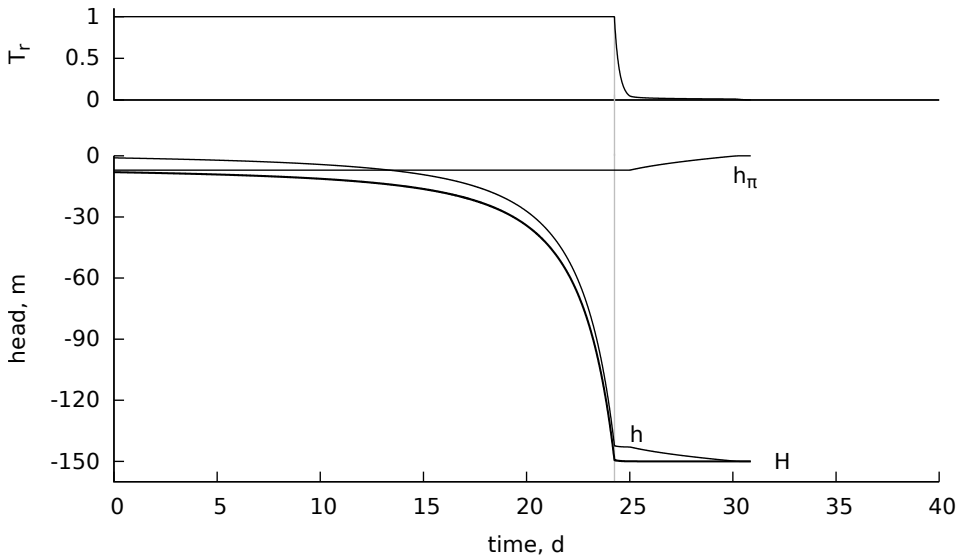

Figure 14 - Pressure (h), osmotic (h_π) and total hydraulic (H) heads at the root surface as a function of time predicted by the non-linear (NLU) uptake model, for scenario 1

Figure 15 shows the solute uptake rate (solute flux at the root surface q_{s_0}) as a function of time for each model. It shows the three uptake phases for NLU (LUP, CUP and NUP), the constant uptake rate for CU, and the zero uptake rate for ZU, according to their respective boundary conditions. This figure shows that, during the LUP phase the solute uptake rate is higher than during CUP and NUP due to the constant potential transpiration rates and the absence of a plant controlled mechanism of solute uptake. This result is in agreement with the model assumption 1, stating that the plant does not control the solute taken up by mass flow of water. Similar result were found by

Šimunek and Hopmans (2009) in simulations using a macroscopic model that considers active and passive uptake of solutes. Their predictions resulted in high solute uptake rates at high concentrations when passive uptake was occurring (their Figure 12), with a concave reduction of uptake with decreasing solute concentration, as shown in Figure 15. Additionally, Robinson (1994) concluded, in his review, that there is no limit for the uptake of some ions like NO_3^- and K^+, making the predictions of the model plausible. However, the model does not consider any mechanism of solute uptake regulation for the high concentration range. These results, therefore, need confrontation with experimental data of solute uptake of non-stressed plants to verify whether a plant regulated mechanism of uptake should be considered. Data of this type can be found in Robinson (1994) and in De Willigen and Van Noordwijk (1987).

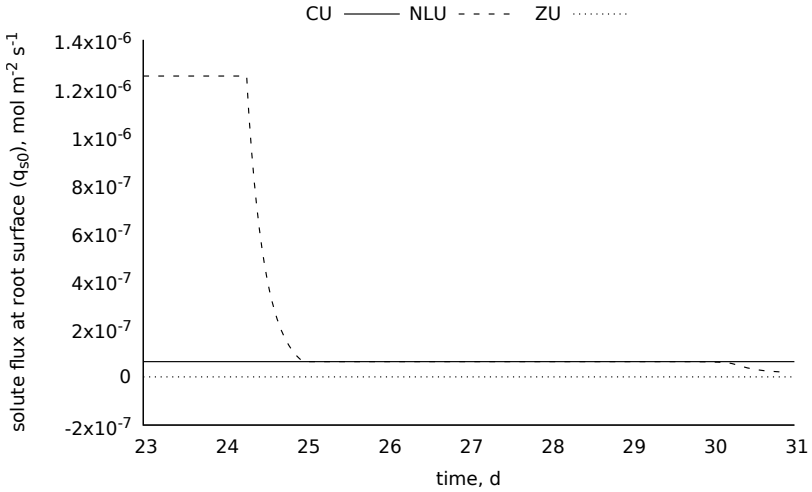

Figure 15 - Detail of solute flux at the root surface as a function of time for constant (CU), zero (ZU) and non-linear (NLU) uptake models, for scenario 1

The predicted cumulative amount of solute extracted by the plant is shown in Figure 16. It can be interpreted as the amount of solute accumulated inside the plant. The high uptake rate at LUP, according to the NLU model, causes a fast accumulation of solute inside the plant due to passive uptake. According to the model assumptions, the plant does not regulate passive uptake (or the uptake caused by mass flow of water), which, for the case of NLU model in all simulated scenarios, is the greatest contribution to the uptake. The ZU model, due to its boundary conditions, does not accumulate any solute and the LU model accumulates solute, at a constant rate.

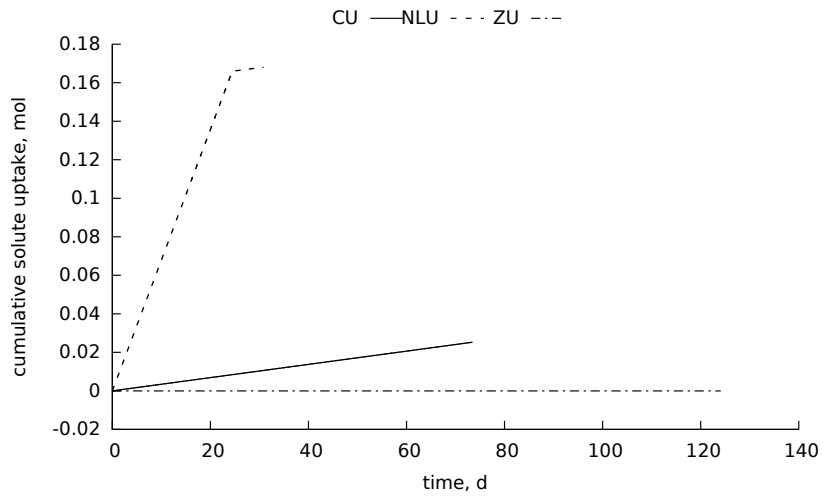

Figure 16 - Cumulative solute uptake as a function of time for constant (CU), zero (ZU) and non-linear (NLU) uptake models, for scenario 1

The CU model may show a phase with accumulation of solute near the root surface depending on the potential transpiration rate and solute uptake rate values. This phase is then followed by a phase of diffusion of solute away from the roots which, together with the solute uptake, are responsible for the depletion of solute at the root surface. This behavior causes a different predicted solute concentration profile at completion of simulation when compared with the proposed solute uptake model (NLU). However, CU and NLU models predict similar concentration profiles when the value of I_m for CU model is increased. This is shown in Figure 17 for the CU model for an arbitrary chosen tenfold higher uptake rate. Predictions of concentration profiles of CU and NLU are close, with differences due to the diffusion of solute away from the roots, resulting from the solute accumulation phase that generates a higher concentration somewhere between r_0 and r_m at completion of simulation. It is also shown that the models that consider solute uptake (CU and NLU) present a smaller concentration at r_m due to the higher solute transport towards the root generated by the gradient caused by the solute uptake at r_0.

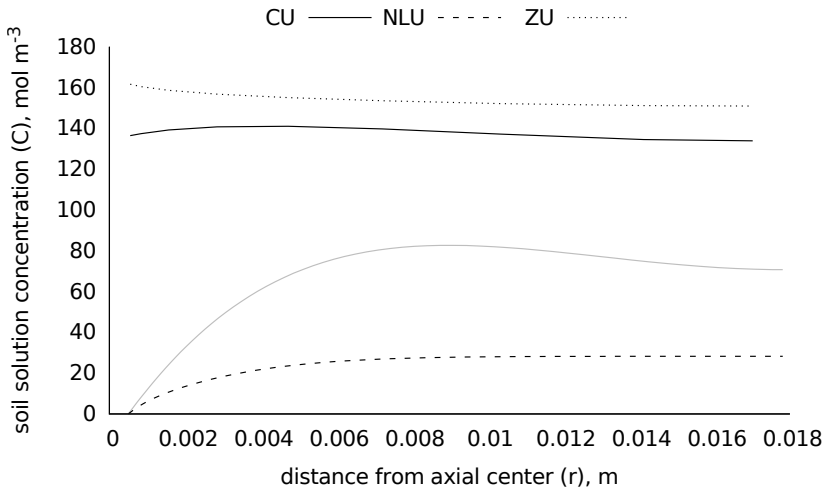

Figure 17 - Soil solution concentration as a function of distance from axial root center at completion of simulation for constant (CU), zero (ZU) and non-linear (NLU) uptake models. Gray line is CU with an arbitrary chosen 10 times higher value for the constant of solute uptake rate ($I_m = 2 \cdot 10^{-5}$ mol cm^{-2} s^{-1})

5.3 Model results

After analysis of solute uptake predictions by the linear (LU) and non-linear (NLU) uptake model discussed in Section 5.1, the simulations of scenarios 1 to 8 (Table 4) were performed using the NLU model. Simulation results for these scenarios are shown in Figures 18 to 23. All simulations started at pressure head (h_{ini}) of -1 m, so that both wet and dry soil conditions occurred in the simulated period. In this section, the results of the main output variables ($C_0(t)$, $C(r)$ and $T_r(t)$) are presented for each scenario, as well as the predicted active and passive contributions to solute uptake.

5.3.1 Concentration at the root surface as a function of time $C_0(t)$

For the simulation scenarios, the set of input parameters h_{ini} and C_{ini} were chosen for the simulations to start always at LUP, when relative transpiration $T_r = 1$ and solute uptake occurs by mass flow of the solution only (passive uptake). In this phase, the water content and concentration in bulk soil deplete at the same rate, resulting in a phase of constant solute concentration. Results from these simulations are shown in Figure 18 for scenarios involving different textures (different soil hydraulic properties), different root length densities, different initial solute concentrations and different potential transpiration rates. For different soil types, although the initial concentration in bulk soil is the same (10 mol m^{-3}), initially, the predicted concentrations at the root surface are different, as shown in Figure 18a. This occurs because the initial condition refers to a fixed pressure

head, resulting in different water contents for each soil in accordance to their hydraulic parameters.

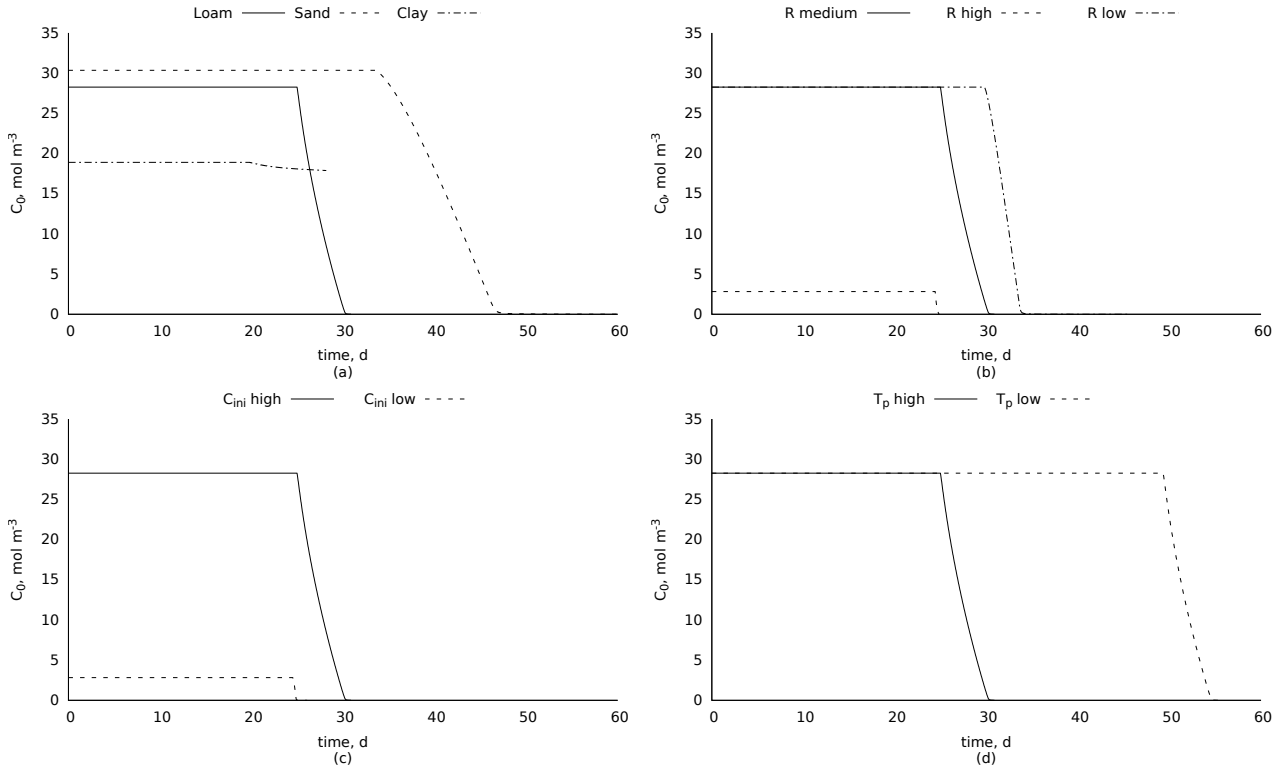

Figure 18 - Solute concentration in soil water as a function of time predicted by the non-linear uptake model (NLU) for scenarios differing in (a) soil hydraulic parameters (according to texture class), (b) root length density, (c) initial solute concentration, and (d) potential transpiration rate

The constant uptake phase (CUP) is characterized by the depletion of C_0 at a constant rate, which starts some time after the onset of the T_r falling rate phase, as shown in Figure 19. The reduction in q_0 (reflected in T_r) increases C_2 value according to Equation (31), therefore, the time that CUP initiates depends on the rate at wich q_0 decreases, which changes with soil type, root density, initial concentration and potential transpiration (Figure 18).

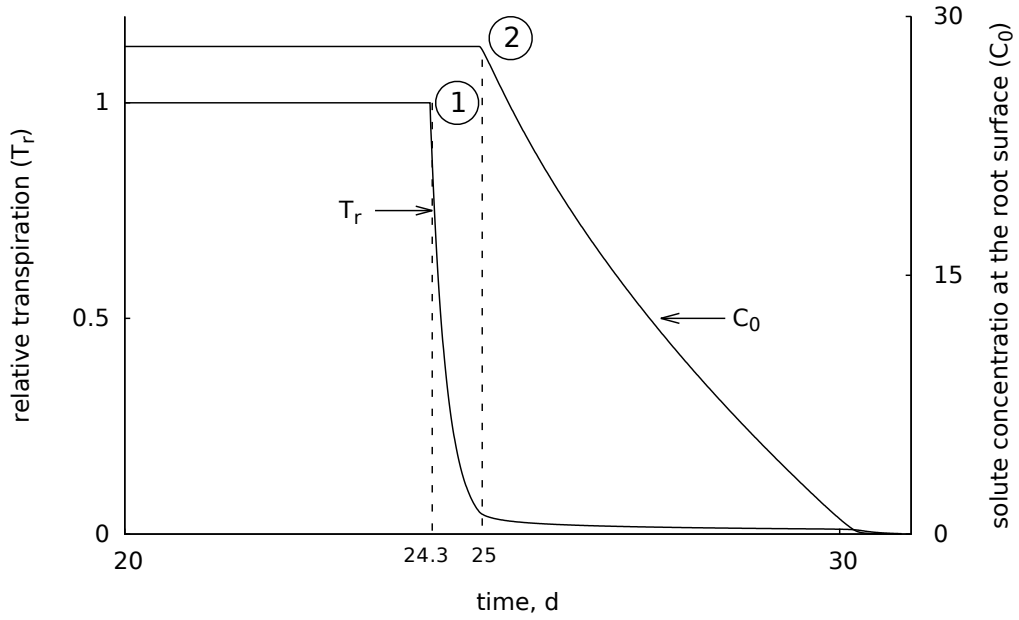

Figure 19 - Relative transpiration and solute concentration at the root surface as a function of time predicted by the non-linear model for scenario 1. (1) indicates the onset of the T_r falling rate phase and (2) indicates the onset of the C_0 falling rate phase

5.3.2 Active and passive uptake

Predictions of active and passive contributions as a function of time and concentration in soil solution are shown respectively in Figures 20 and 21, according to Equation (29) and the model assumptions. From the onset of simulations (wet condition, $T_r = 1$), although scenarios start in LUP, a constant (instead of a linearly decreasing) uptake rate is developed. This is due to the fact that the model considers a constant potential transpiration rate over time, therefore, the solute uptake is determined by (constant) water flow q_0 and solute concentration C_0 (Equation (29.3)), also constant because passive uptake by mass flow is the dominating process. The constant concentration in soil solution also occurs in the simulations of Šimunek and Hopmans (2009) when only passive uptake is considered. A plant controlled scenario allowing the reduction of solute uptake including, for example, a reflection coefficient that accounts for the effectiveness of exertion of osmotic pressure of a solute across a membrane (NOBEL, 1999) might be a modeling alternative to describe controlled uptake in this phase. In our model such a feature was not included and, according to model assumptions, LUP includes a constant solute uptake rate phase in which the uptake rate depends on the potential transpiration, soil hydraulic properties, root length density, and initial solute concentration. It does not depend on ion type, since q_{s_0} values were equally predicted (Figure 20).

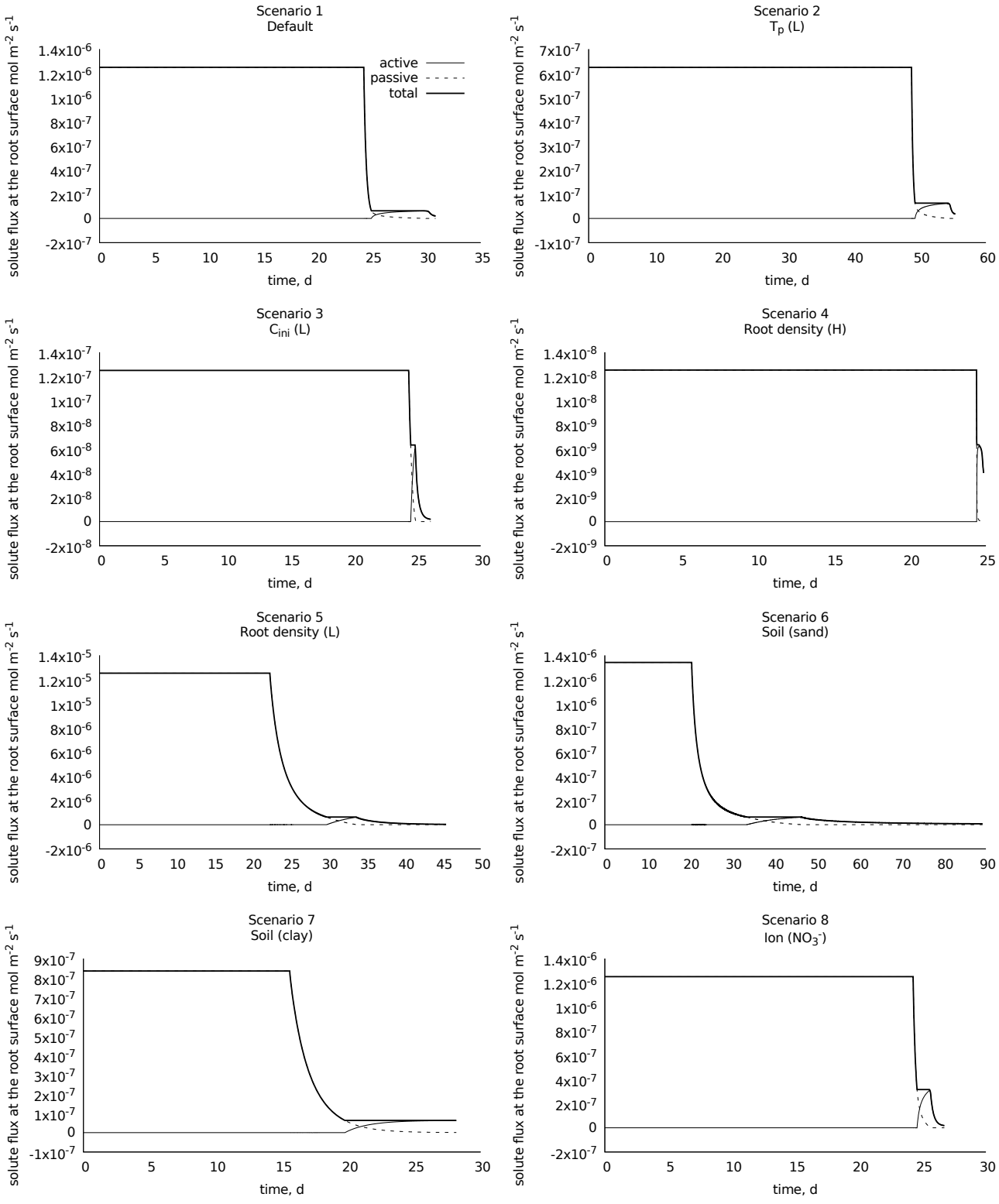

Figure 20 - Active and passive contributions to the solute uptake as a function of time predicted by NLU. Bold line represents the total solute uptake (active+passive), the thin line represents active contributions to the solute uptake, and the dashed line represents the passive contribution. Simulated scenarios according to Table 4

During the CUP, the solute uptake by mass flow (passive uptake) does not attend completely the plant demand (Figure 11), thus, according to the model assumptions, an

active uptake develops which becomes higher as passive uptake becomes lower in order to maintain the constant uptake rate. It is a different approach than that of Šimunek and Hopmans (2009) who use the assumption of independent responses of active and passive uptake. In the proposed model, the constant demand at CUP, composed by active and passive uptake, is maintained until C_0 reaches C_{lim} which, in turn, increases as q_0 decreases, according to Equation (30). Active uptake reaches its maximum value when $C_0 = C_{lim}$ and the uptake is then limited by the concentration in the soil in further time steps, starting the non-linear uptake phase (NUP). It can be seen in Figure 20 that the time of the occurrence of the maximum value for active uptake depends on the rate by which passive uptake decreases, equal to the rate of decrease of q_0 and C_0, depending on the rate of solute uptake I_m according to Equation (29) and model assumptions. Therefore, the soil type, root density, initial concentration, and potential transpiration also affects the time for the maximum active uptake value and, consequently, the time at which NUP starts.

An important feature of the non-linear uptake phase (NUP) is a second falling rate phase for T_r (as shown in Figure 6). The total hydraulic head H is not allowed to decrease below H_{lim} and, as the solute uptake rate (q_{s_0}) decreases due to the limitation imposed by C_{lim} (Equation (29)), a decrease in the water uptake rate (q_0) is predicted in order to maintain H at its limiting value. This phase is of very short duration as it starts with very low values of q_0 and T_r, near the completion of simulations at $T_r = 0.001$, when q_0 is considered negligible. In this phase, however, the active component of uptake dominates, being the major component of the solute uptake.

Different predictions for the active and passive contributions for solute uptake as a function of solute concentration are shown in Figure 21. Modifying T_p from the low to the high rate cause a change in the length of the phases (LUP, CUP and NUP), but no alteration in the active and passive partitioning was predicted. This result is straightforward since the potential transpiration affects the rate of the potential water flux and water uptake which, on their turn, affect the rate of solute uptake. Keeping soil hydraulic properties, root length density, ion type and solute uptake parameters the same, similar results are expected, although on a different time scale. The most significant alteration in the partitioning between active and passive uptake is predicted when changing hydraulic properties (especially for the clay soil) and root length density values (Figure 21).

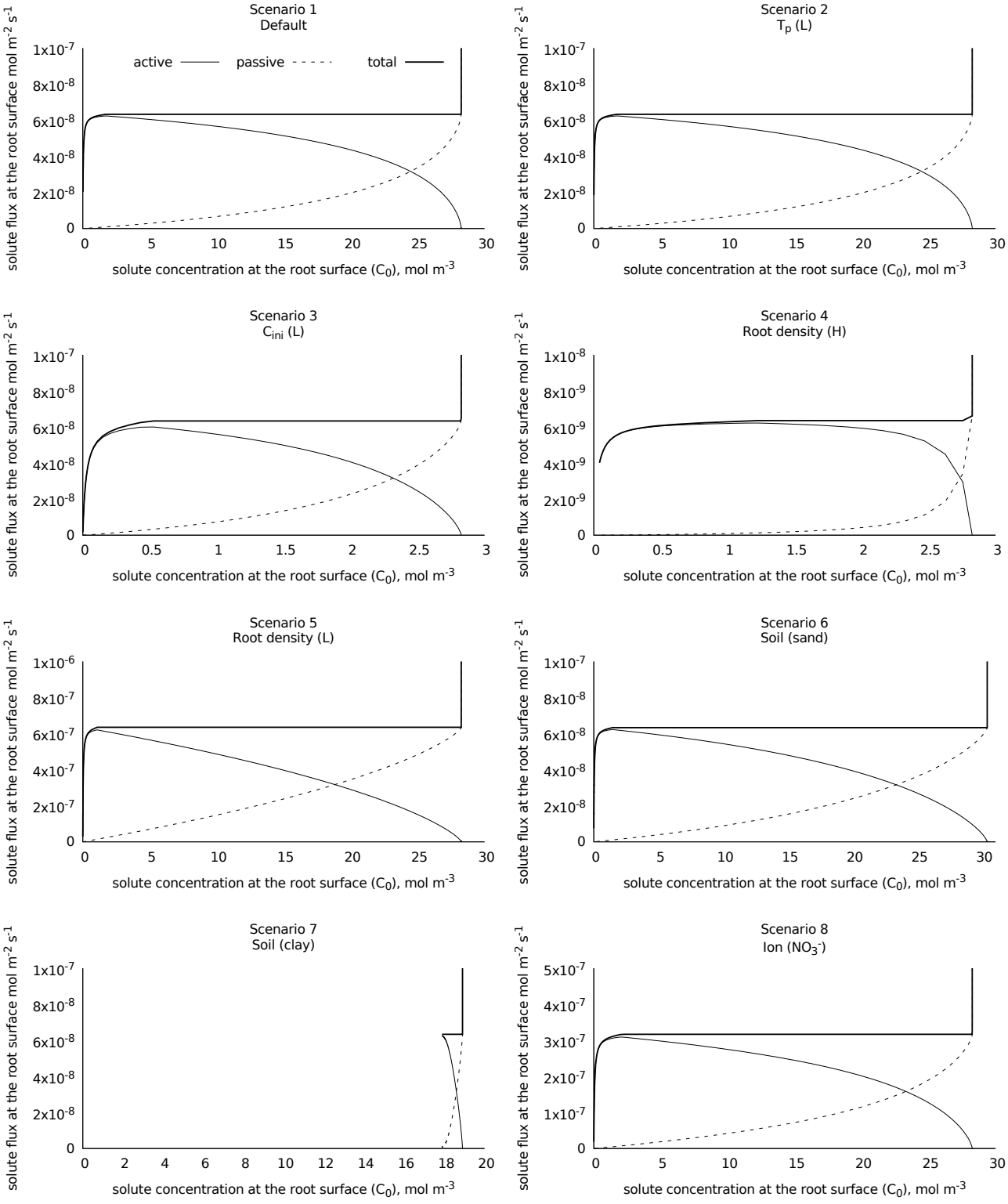

Figure 21 - Active, passive and total uptake as a function of solute concentration. Bold line represents the total solute uptake (active+passive), the thin line represents active contributions to the solute uptake, and the dashed line represents the passive contribution. Simulated scenarios according to Table 4

In the clay soil, the solute uptake is smaller due to the smaller initial concentration calculated in agreement with its hydraulic parameters. The low hydraulic conductivity

of this soil makes the limiting potential H_{lim} to be reached in an earlier phase, reducing the time to the onset of the T_r falling rate phase and, consequently, the uptake caused by the convective transport (passive uptake). As a result, the diffusive transport (active uptake) quickly becomes dominant at the root surface (Figure 21, scenario 7).

At high root densities, more water is extracted from the same soil volume during a given period, causing a delay in the onset of T_r reduction. The higher root length density leads to a steeper falling rate phase (Figure 23). Therefore, active uptake becomes more important with increasing R, as can be seen in Figure 21 (scenarios 1, 4 and 5). This modeling result is in agreement to the simulations performed by De Jong van Lier, Metselaar and Van Dam (2006) who show the time of first occurrence of limiting water potential increasing with higher root densities.

5.3.3 Concentration profile $C(r)$ and relative transpiration $T_r(t)$

The final concentration profile and relative transpiration are important modeling results. The former is essential to determine the gradient of solute concentration and fluxes. Additionally, it can be used to compute the average solute concentration in a soil layer, important for model upscaling since it is required for one-dimensional macroscopic models. The latter is used to predict water and osmotic stress, which can be related to biomass accumulation and yield predictions. Figure 22 shows that, at the final time step of simulations, the concentration profiles and profile average solute concentration are affected by all selected parameters, except potential transpiration. As expected, a change in T_p causes changes only in the time at which C_0 reaches limiting values (C_2 and C_{lim}) due to the decrease in water and solute fluxes. Corroborating with these results, Figure 21 shows the same amount of active and passive uptake contributions, according to the actual concentration in the soil, for both scenarios 1 ($T_p = 6$ mm) and 2 ($T_p = 3$ mm), whereas the T_r falling rate phase onsets earlier when T_p is increased (Figure 23). In other words, these simulations show that a reduction of T_p results in the same predicted solute concentration profiles, but at a different time scale.

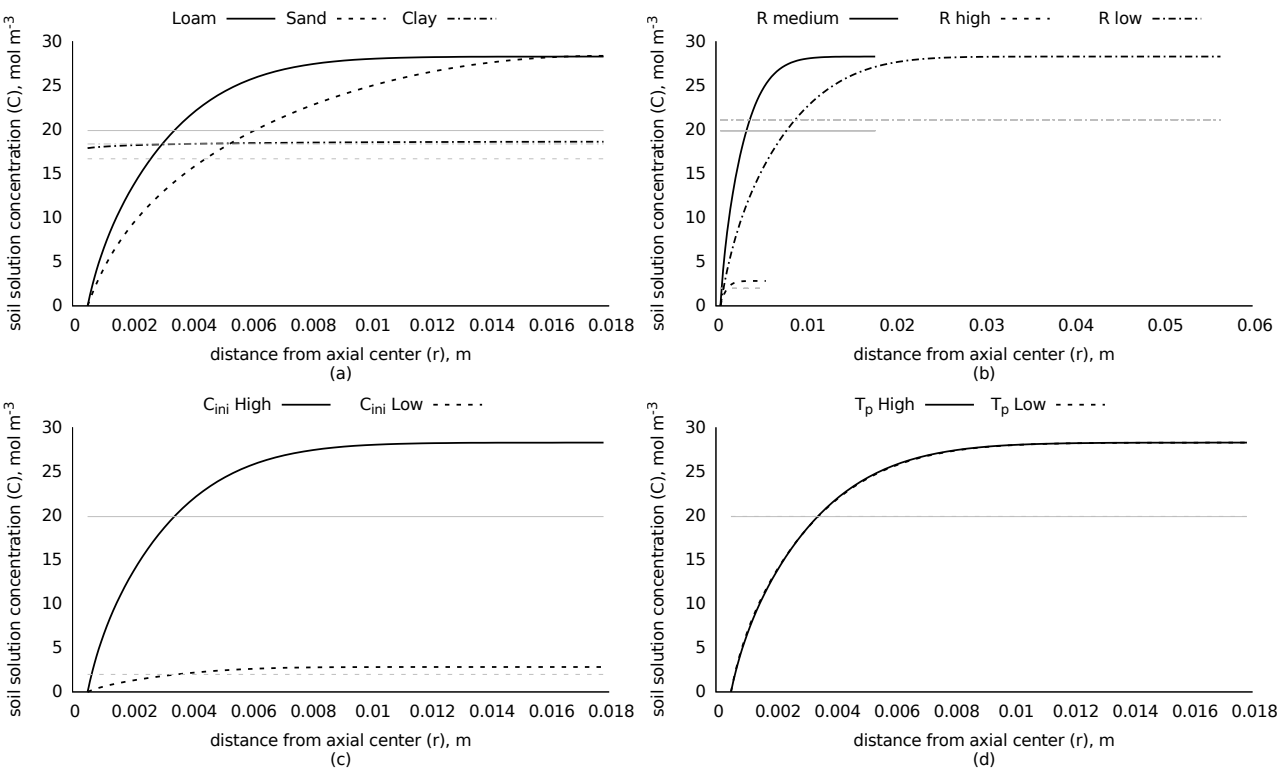

Figure 22 - Solute concentration in soil water as a function of distance from axial center simulated at completion of simulations, for different scenarios regarding (a) hydraulic properties, (b) root length density, (c) initial solute concentration, and (d) potential transpiration. Thin lines indicates the average concentration

Soil hydraulic properties and root length density change the final concentration profile respectively due both to the different soil hydraulic properties that affect water movement and to the greater water and solute uptake per soil volume unit (see earlier discussion in Section 5.3.2). Similarly, they affect the steepness of the T_r falling rate phase, also modifying the length of the phases LUP, CUP and NUP. The initial concentration, for obvious reasons, changes the final concentration profile as well. It slightly changes the onset of falling T_r rate phase due to the osmotic hydraulic head component. These results, showed in Figure 23, are in accordance to the findings of De Jong van Lier, Van Dam and Metselaar (2009) model which states that the onset of the falling T_r rate phase is a function of potential transpiration, solute initial concentration and root density. The highest variation caused by changes in initial concentration can be observed in CUP and NUP. With low values of C_0 (h_π closer to zero), H_{lim} is achieved faster because there is less solute in soil to be taken up. This causes a steeper T_r reduction curve, shortening the time needed to C_0 be smaller than C_{lim} (condition that onsets NUP).

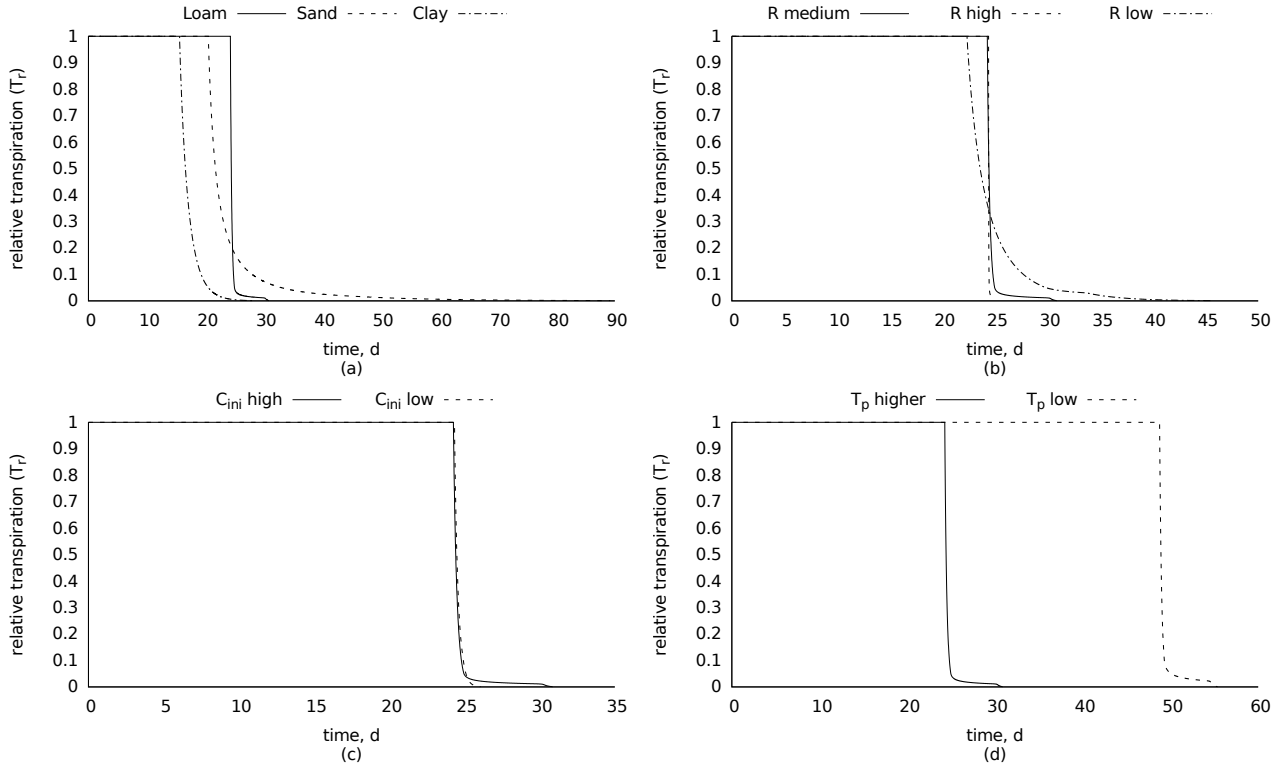

Figure 23 - Relative transpiration as a function of time, predicted for different scenarios referring to (a) hydraulic properties, (b) root length density, (c) initial solute concentration, and (d) potential transpiration

5.3.4 General comments on model results

Figures 20 and 21, referring to scenarios 1 to 7, show that with the same values of I_m and K_m (same solute), different sets of active and passive contributions can be observed just due to changes in soil, root and atmospheric parameters. Different than simulated scenarios, real systems soil water contents changes due to rain or irrigation, the solute concentration may be altered by the addition of nutrients to the soil, and the atmospheric demand is far to be constant. The variation of all model parameters due to the natural changes that occur in a real system would generate a wide range of different responses of root uptake and its passive and active contributions, being hard to be predicted even with a more complex model. This reveals the system complexity to be simulated and how much is still missing to come to a more complete understanding of the dynamics of these phenomena.

The partitioning of the solute uptake in active and passive processes, as simulated by the model, may increase insight and lead to further studies. It reveals about the metabolic partitioning of energy used by the plant that regulates solute uptake, which

would be useful to predict its stress status and separates osmotic and ionic stressors. To improve results, the uptake model should be coupled to a more complex plant model, which deals with metabolic processes as a function of the solute concentration within plant cells (nutritional status) and time. Separating osmotic and ionic stress would lead to more detailed predictions of crop stress, growth and yield. Besides, it also could be useful to water and nutritional management.

5.4 Sensitivity analysis

To better analyze the impact of the variation of the model input parameters, a sensitivity analysis is presented in this section.

The relative partial sensitivity η is the fraction of the relative change in parameter P that will propagate in a model prediction Y (DE JONG VAN LIER; WENDROTH; VAN DAM, 2015). For example, $\eta = 0.5$ means that a 1% increase of P results in 0.5% increase in the prediction Y. The value of η found through a variation of a parameter is likely to change with variation of another parameter, making a sensitivity analysis that deals with all combinations of parameters variation of a complex model being profoundly difficult to be done. Therefore, the analyses are commonly restricted to a fixed set of parameters (DRECHSLER, 1998).

Besides modeling results expressed as solute concentration as a function of time and distance ($C(r,t)$), the model can give a wide range of another predictions. For instance: relative transpiration, pressure and osmotic potentials, water and solute uptake rates, and accumulated solute uptake. Some of these predictions were selected to check how changes in soil and ion/plant parameters would affect them. The selected predictions Y were: time to completion of simulation (t_{end}), osmotic head (h_{os}), time at the onset of the T_r falling rate phase (t_{T_r}), time at the onset of constant uptake phase (t_{C_0}) and accumulated solute uptake (acc). Varying parameter P were the ion/plant (I_m and K_m) and the soil hydraulic parameters (α, n, K_s, λ, θ_r and θ_s).

Sensitivities to ion/plant parameters were high for h_{os} and presented an inverse response (negative values) to I_m variation (Figure 24). This is because, with higher values of I_m, solute uptake rates are higher in both constant and non-linear uptake phases, diminishing the value of the concentration at the root surface simulated at the completion of simulation (less negative values of osmotic head h_π). On the contrary, higher values of K_m correspond to higher values of C_{lim} causing an increase of the non-linear uptake phase and a decrease in the constant uptake phase. With less time of potential solute

uptake, the final concentration increases due to a lower amount of extracted solute. Thus, in general, a variation of 1% in K_m and I_m results in, respectively, a decrease of 1.2% and an increase of 1%, approximately, in h_{os}. The exception to this tendency was scenario 7 that showed low η values for both parameters. The reason for this different behavior is the small variation in C_0 during the simulation due to the low water and solute fluxes of the clay soil, as commented in the previous section.

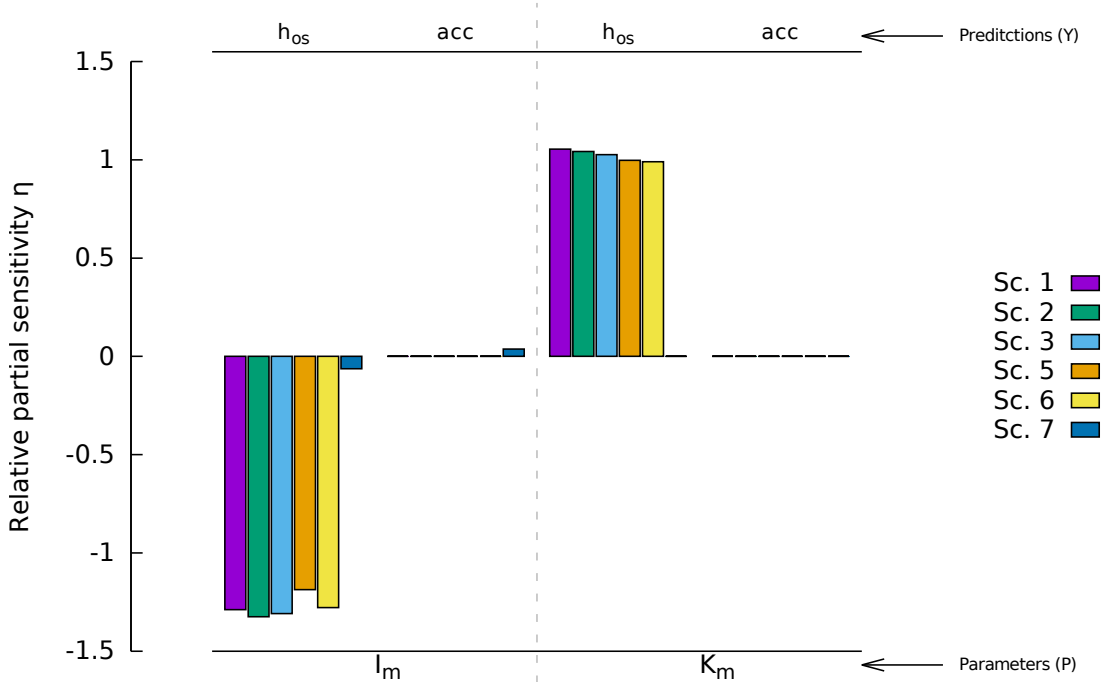

Figure 24 - Relative partial sensitivity of osmotic head at the root surface simulated at completion of simulation (h_{os}) and accumulated solute uptake (acc) to MM equation parameters I_m and K_m for scenarios 1 to 7

Figure 24 shows that, despite the sensitivity of h_{os}, acc shows very low (close to zero) sensitivity to K_m and I_m. This is because I_m and K_m affect the solute uptake rate only in the constant and non-linear uptake phases, since all the uptake in the linear uptake phase is due to mass flow of water. The constant and non-linear phases are relatively short when compared to the linear phase, making the influence of I_m and K_m on the accumulated solute uptake to be low.

Figure 25 shows low sensitivity of the time related predictions to I_m and no sensitivity to K_m. As the model deals with constant potential transpiration only, the time at the onset of the T_r falling rate phase is the exact time when q_0 starts to decrease. I_m and K_m do not exerts any influence in this phase, which explains the zero sensitivity of t_{T_r} to those parameters.

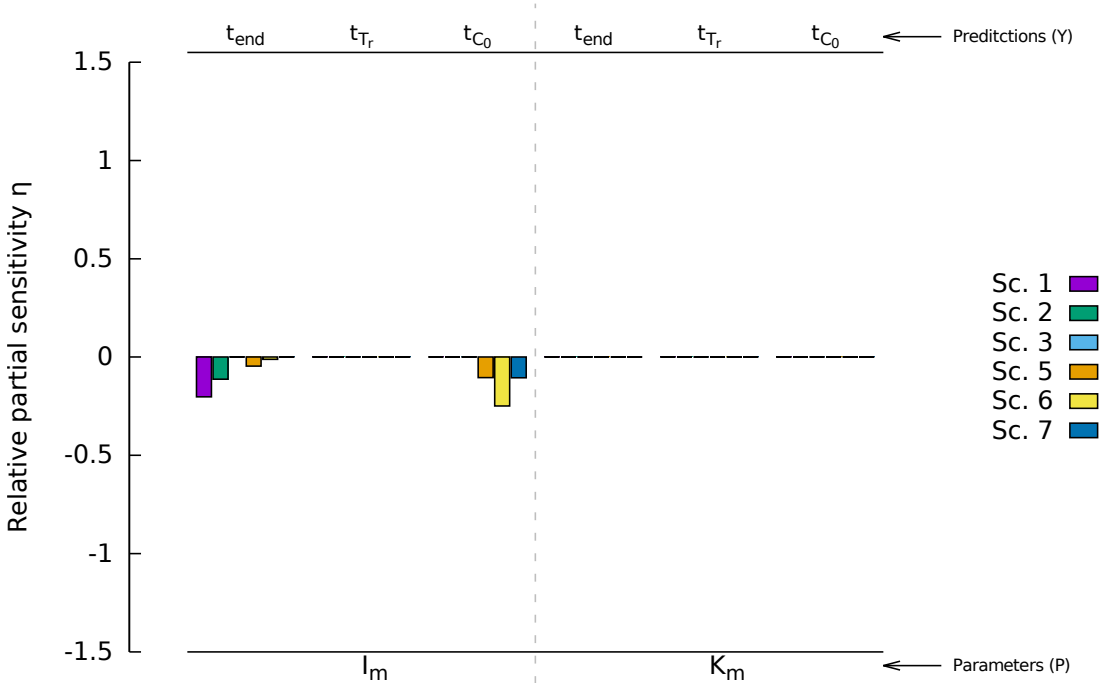

Figure 25 - Relative partial sensitivity of time to completion of simulation (t_{end}), time at the onset of the T_r falling rate phase (t_{T_r}) and time at the onset of constant uptake phase (t_{C_0}) to MM equation parameters I_m and K_m for scenarios 1 to 7

The predictions for t_{end} and t_{C_0} presented low sensitivity to I_m and no sensitivity to K_m. I_m is directly related to the solute uptake rate (as it defines the plant demand) and K_m to the C_{lim} value. Thus, higher values of I_m causes higher uptake rates, faster decrease of water and solute contents and, therefore, a faster decrease of T_r and a earlier completion of the simulation.

Figures 28, 29 and 26 show the sensitivities to the soil hydraulic properties. Although the sensitivity results are presented separately for each parameter, output and scenario, the interactions between all parameters and simulated processes occur synergistically and concomitantly. Due to the relative nature of the sensitivity (there is no absolute value of η for one prediction with a variation of different parameters), an individual analysis can give insight in the importance of a parameter to the model, but it only represents the specific scenario. Therefore, due to the high number of soil hydraulic parameters, the discussion will focus on those parameters with the highest η values.

Parameter n showed the highest (absolute) values of η among the soil hydraulic properties, mainly for h_{os} at completion of simulation, yielding as negative as -23 for scenario 2 (Figure 26). A similar result was found by de Jong van Lier, Wendroth and van Dam (2015), whose yield predictions of the evaluated model showed the highest sensitivity for the n parameter. Figure 27 shows how the water retention curve (a) and

the hydraulic conductivity (b), following the Van Genuchten (1980) model, are affected by the n parameter.

Parameter n affects both water retention and hydraulic conductivity. An increase in this parameter causes a steeper decrease in both hydraulic functions. The same value of water content corresponds to a higher (more negative) values of pressure head. Increasing n makes the solute uptake rate to increase because the same initial pressure head originates lower values of water content and, consequently, higher solute concentration values. Therefore, due to the higher solute uptake rate, the limiting value H_{lim} is reached at later times, extending LUP and resulting in less negative values of solute concentration in soil water (h_π), as in the simulations with loam soil (scenarios 1, 2, 3, 4 and 5). Nevertheless, despite the higher change in the water retention curve for the clay soil it does not affect the η value of scenario 7 in the same proportion. Due to the interactions between water retention and hydraulic conductivity curves, the overall effect is difficult to be properly analyzed without an empirical test. However, the lower value of η in scenario 7 may be caused by the fact that the solute uptake rate in this scenario is very low. Therefore, even with a variation of 1% in n causing a change in the retention curve (and consequently in the concentration values), it does not strongly affect the solute uptake rate and, consequently, the change in h_π (or h_{os}) at completion of simulation is small.

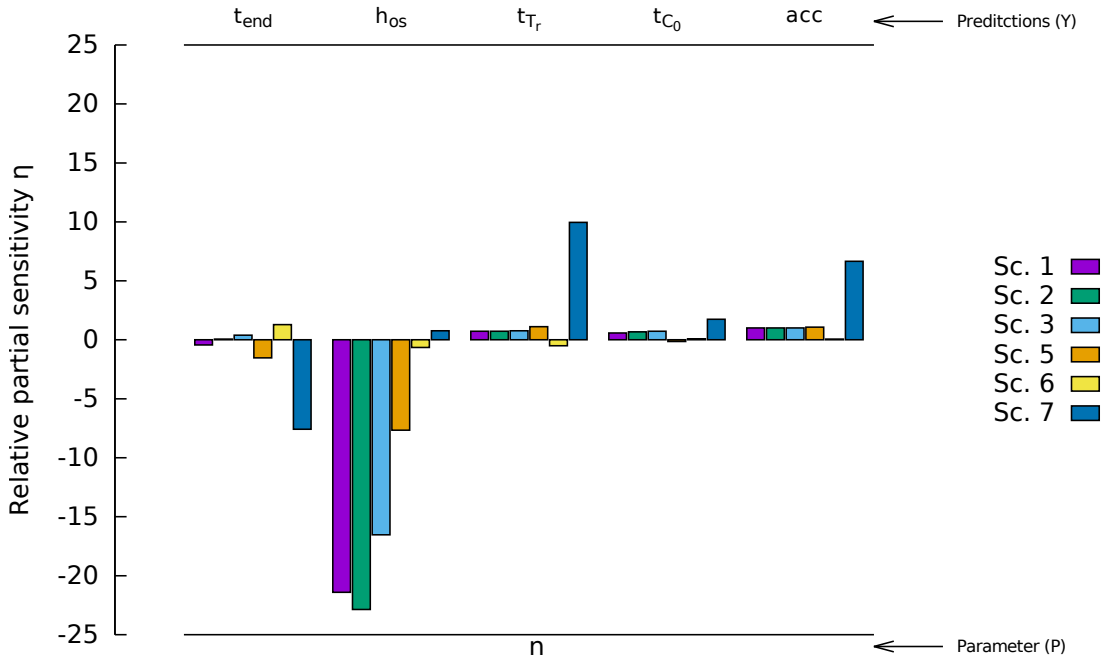

Figure 26 - Relative partial sensitivity of time to completion of simulation (t_{end}), osmotic head (h_{os}), time at the onset of the T_r falling rate phase (t_{T_r}), time at the onset of constant uptake phase (t_{C_0}) and accumulated solute uptake (acc) to soil hydraulic parameter n for scenarios 1 to 7

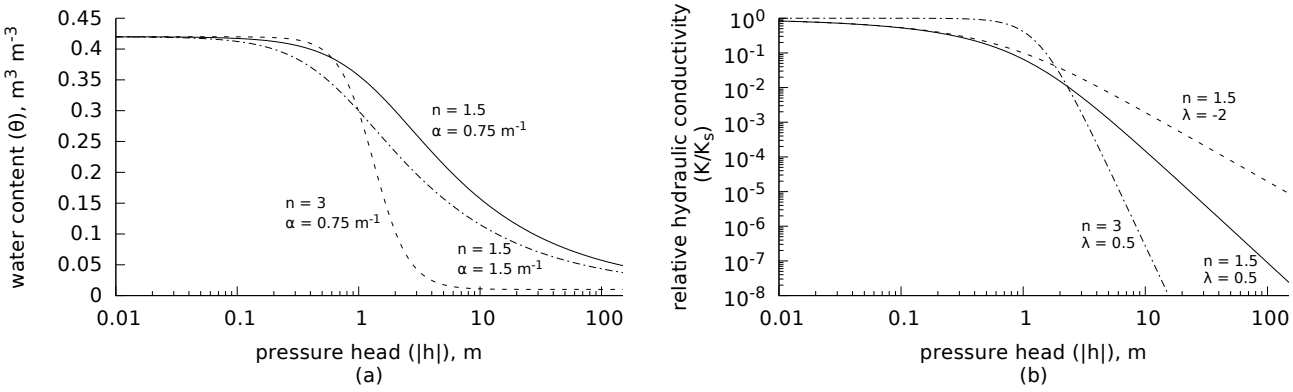

Figure 27 - (a) Water content from Equation (10), for three combinations of α and n, and (b) relative hydraulic conductivity from Equation (11) for three combinations of λ and n, with $\alpha = 0.75$ m^{-1}

For the predictions at specific times (t_{end}, t_{T_r} and t_{C_0}), the parameters θ_s and λ presented the highest (absolute) η values. Increasing values of θ_s increases the available water content and increases at about the same proportion ($\approx$1%) t_{T_r}, t_{end} and t_{C_0} due to an extended period of water uptake at T_p. Parameter λ affects the shape of the hydraulic conductivity function. A higher λ results in a steeper decrease of hydraulic conductivity with water content (Figure 27b), extending the period of water uptake at potential levels increasing the time to the onset of T_r falling rate phase (t_{T_r}). On the other hand, the steeper decrease in hydraulic conductivity causes a more intense decrease in the water flux which, on its turn, decreases the time to completion of simulation (t_{end}) value (Figure 28). The higher sensitivity to θ_s can be explained due to the fact that the model has a powerful (possibly overestimated) solute extraction at the LUP, either due to the absence of a plant regulated process for solute uptake at this phase or because the model does not consider a regulation in the solute uptake according to solute concentration inside the plant.

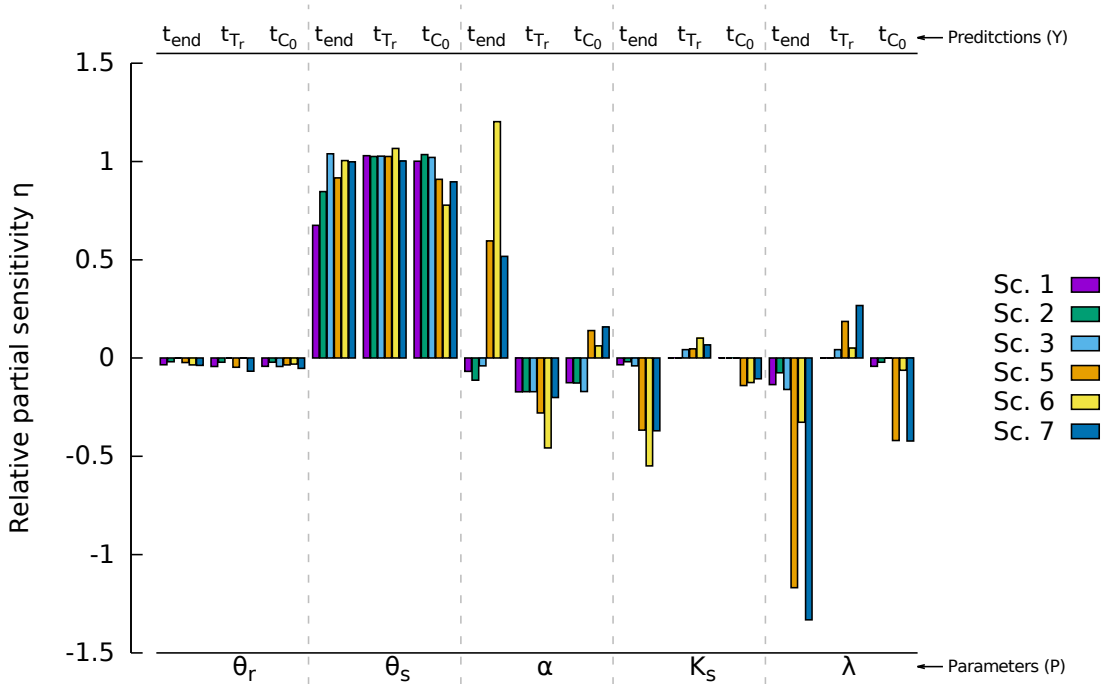

Figure 28 - Relative partial sensitivity of time to completion of simulation (t_{end}), time at the onset of the T_r falling rate phase (t_{T_r}) and time at the onset of constant uptake phase (t_{C_0}) to soil hydraulic parameters θ_r, θ_s, α, K_s and λ for scenarios 1 to 7

For the solute related predictions, h_{os} showed high sensitivities to θ_r, θ_s and α (Figure 29). The sign of sensitivity of h_{os} to θ_r and θ_s is straightforward. An increase in θ_r decreases the available water content, shortening the LUP phase and t_{T_r}. As a result, the highest solute uptake rate phase is reduced causing, at completion of the simulation, a higher solute concentration at the root surface (more negative h_{os}). On the other hand, an increase in θ_s causes an increase in the available water content, extending LUP which results in a lower solute concentration at the root surface (less negative h_{os}). As the change in the retention curve is similar to the variation of n, the effects are also similar. At completion of simulation values of h_π are lower due to the higher solute uptake rate. On its turn, parameter α affects the shape of the water retention curve by changing the air entry pressure head. An increase in its value makes the same water content to correspond to a less negative pressure head (Figure 27a).

Accumulated solute uptake at completion of simulation (acc) presented the lowest sensitivity to all parameters for almost all scenarios. As the major part of solute uptake occurs during LUP (the initial phase, when $C > C_2$), acc is most affected when the duration of this phase is altered. The sensitivity of t_{T_r} serves as an indicator to the duration of this phase, in a way that acc responds more strongly when t_{T_r} is also affected.

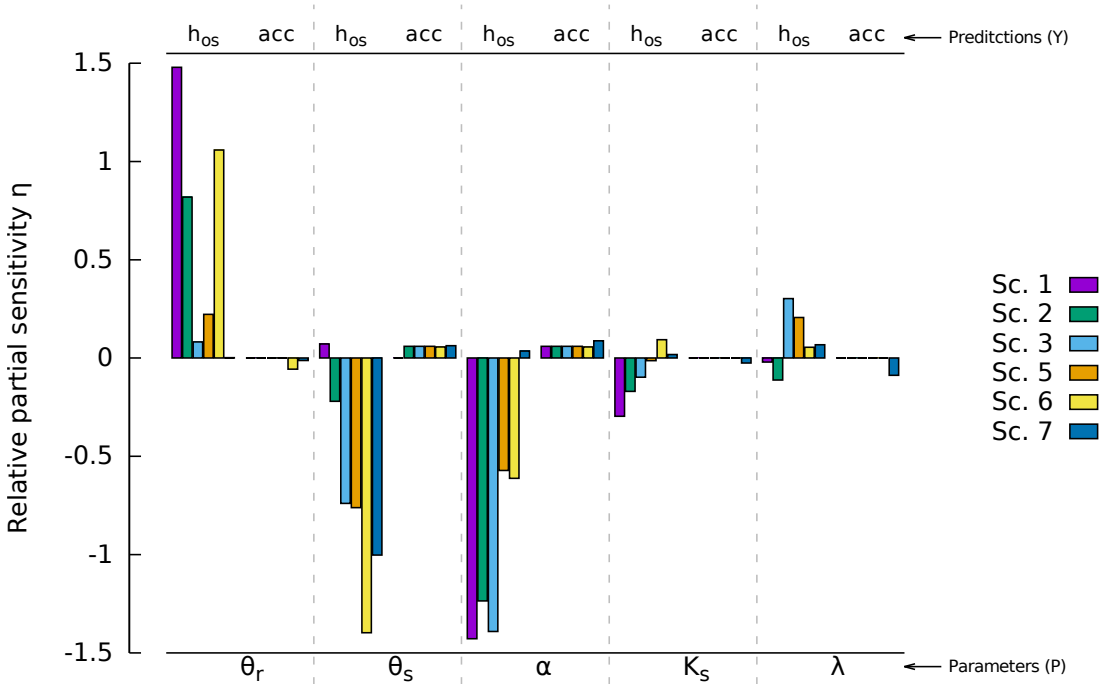

Figure 29 - Relative partial sensitivity of osmotic head at the root surface at completion of simulation (h_{os}) and accumulated solute uptake (acc) to soil hydraulic parameters θ_r, θ_s, α, K_s and λ for scenarios 1 to 7

5.5 A final remark

Although the model showed acceptable results, it needs more testing with different scenarios and its results need to be confronted with experimental data to check for discrepancies and flaws. There are a number of other models (analytical and numerical) developed with the same purpose, each of them with its deficiencies. Simulating a natural phenomenon is always limited by the human knowledge, by the way he observes and deduces. Therefore, this particular model is just one of the possible (and limited) ways to simulate the complex processes that occur in the SPA system, narrowed by the implicitly limited knowledge of its author and, thus, should be used with caution.

6 CONCLUSIONS

The partial differential equation of convection-dispersion was numerically solved using a fully implicit scheme, considering a transient state of solute flow and a solute uptake rate that is dependent on the solute concentration in the soil. This solution was then incorporated into the model of De Jong van Lier, Van Dam and Metselaar (2009) including the root solute uptake. The resulting model has a linear and a non-linear solution for the solute uptake equation and shows a good agreement with the analytical solution proposed by Cushman (1979) which also considers a concentration dependent uptake as the boundary condition at the root surface. The linear and non-linear solutions are significantly different only when comparing the concentration as a function of time for times where $C_0 < C_{lim}$ (non-linear uptake phase, NUP).

Simulations results show that a second reduction in the relative transpiration may occur by a reduction of the solute uptake rate resulting in a reduction of water flux due to the decreasing value of pressure head needed to maintain the limiting value of $H = H_{lim}$. This second reduction shows that the limiting value C_{lim} can be an important parameter to determine changes in the combined water and osmotic stress in low concentration situations, suggesting it requires more investigation.

The model showed able to be able to quantify the active and passive contributions to the solute uptake, which can be used to distinguish osmotic and ionic stressors in further works. Soil hydraulic properties, root length density, initial concentration and potential transpiration are factors that change the time that the concentration at the root surface starts to decrease and the time that the active uptake is maximum.

From the sensitivity analysis, we conclude that the quantities requiring a careful parameterization are: θ_r, θ_s, α, I_m and K_m, affecting strongly the solute concentration at the root surface at completion of simulation, θ_s affecting the time at wich limiting values of solute concentration are reached, and n which strongly affects all selected predictions, mainly h_π.

The proposed model uses an implicit scheme for the numerical solution of the convection-dispersion, including variable space steps and diffusion coefficients. A more detailed investigation of stability issues for this kind of model would benefit its applicability and is suggested as a future work.

REFERENCES

BARBER, S.A. A diffusion and mass-flow concept of soil nutrient availability. **Soil Science**, Philadelphia, v. 93, n. 1, p. 39–49, 1962.

_____. Influence of the plant root on ion movement in soil. In: CARSON, E.W. (Ed.). **The plant root and its enviroment**. Charlottesville: Procedures in plant roots and their enviroment, 1974. p. 525–564.

_____. **Soil nutrient bioavailability: a mechanistic approach**. 2 ed. New York: John Wiley & Sons, 1995. 417 p.

BARBER, S.A.; CUSHMAN, J.H. Nitrogen uptake model for agronomic crops. In: ISKANDER, I.K. (Ed.). **Modelling wastewater renovation for land treatment**. New York: Wiley Interscience, 1981. p. 382–489.

BARRACLOUGH, P.B.; LEIGH, R.A. The growth and activity of winter wheat roots in the field: the effect of sowing date and soil type on root growth of high-yielding crops. **The Journal of Agricultural Science**, Cambridge, v. 103, n. 01, p. 59–74, 1984.

BORSTLAP, A. The use of model-fitting in the interpretation of dual uptake isotherms. **Plant, Cell & Environment**, Malden, v. 6, n. 5, p. 407–416, 1983.

BOULDIN, D. A multiple ion uptake model. **Journal of soil science**, Malden, v. 40, n. 2, p. 309–319, 1989.

BRAY, R.H. A nutrient mobility concept of soil-plant relationships. **Soil Science**, Philadelphia, v. 78, n. 1, p. 9–22, 1954.

BROADLEY, M.R.; WHITE, P.J.; HAMMOND, J.P.; ZELKO, I.; LUX, A. Zinc in plants. **New Phytologist**, Malden, v. 173, n. 4, p. 677–702, 2007.

CELIA, M.A.; BOULOUTAS, E.T.; ZARBA, R.L. A general mass-conservative numerical solution for the unsaturated flow equation. **Water resources research**, Washington, v. 26, n. 7, p. 1483–1496, 1990.

CHANTER, D.O. Use and misuse of linear regression methods in crop modelling. In: ROSE, D.A.; CHARLES-EDWARDS, D.A. (Ed.). **Mathematics and plant physiology**. London: Academic Press, 1981. p. 253–267.

CUSHMAN, J.H. An analytical solution to solute transport near root surfaces for low initial concentration: I. equations development. **Soil Science Society of America Journal**, Madison, v. 43, n. 6, p. 1087–1090, 1979.

DALTON, F.N.; RAATS, P.A.C.; GARDNER, W.R. Simultaneous uptake of water and solutes by plant roots. **Agronomy Journal**, Madison, v. 67, n. 3, p. 334–339, 1975.

DE JONG VAN LIER, Q.; METSELAAR, K.; VAN DAM, J.C. Root water extraction and limiting soil hydraulic conditions estimated by numerical simulation. **Vadose Zone Journal**, Madison, v. 5, n. 4, p. 1264–1277, 2006.

DE JONG VAN LIER, Q.; VAN DAM, J.C.; METSELAAR, K. Root water extraction under combined water and osmotic stress. **Soil Science Society of America Journal**, Madison, v. 73, n. 3, p. 862–875, 2009.

DE JONG VAN LIER, Q.; WENDROTH, O.; VAN DAM, J.C. Prediction of winter wheat yield with the swap model using pedotransfer functions: An evaluation of sensitivity, parameterization and prediction accuracy. **Agricultural Water Management**, Amsterdam, v. 154, n. 1, p. 29–42, 2015.

DE WILLIGEN, P. **Mathematical analysis of diffusion and mass flow of solutes to a root assuming constant uptake**. Haren, 1981. 1-56 p. Techinical Report.

DE WILLIGEN, P.; VAN NOORDWIJK, M. **Roots, plant production and nutrient use efficiency**. 282 p. Thesis (PhD) — Wageningen University, 1987.

DE WILLIGEN, P.; VAN NOORDWIJK, M. Mass flow and diffusion of nutrients to a root with constant or zero-sink uptake i. constant uptake. **Soil science**, Baltimore, v. 157, n. 3, p. 162–170, 1994.

DRECHSLER, M. Sensitivity analysis of complex models. **Biological Conservation**, Oxford, v. 86, n. 3, p. 401–412, 1998.

DUDAL, R.; ROY, R.N. **Integrated Plant Nutrition Systems: Report of an Expert Consultation**. Rome: Food & Agriculture Organiztion, 1995. 427 p.

EPSTEIN, E. Spaces, barriers, and ion carriers: ion absorption by plants. **American Journal of Botany**, Saint Louis, v. 47, n. 5, p. 393–399, 1960.

_____. **Mineral nutrition of plants: principles and perspectives.** London: Science Reviews 2000, 1972. 412 p.

EPSTEIN, E.; HAGEN, C.E. A kinetic study of the absorption of alkali cations by barley roots. **Plant physiology**, Rockville, v. 27, n. 3, p. 457, 1952.

FEDDES, R.A.; KOWALIK, P.J.; ZARADNY, H. **Simulation of field water use and crop yield**. Wageningen: Centre for Agricultural Publishing and Documentation, 1978. 189 p.

FEDDES, R.A.; RAATS, P.A.C. Parameterizing the soil–water–plant root system. In: FEDDES, R.A.; ROOIJ, G.H.; VAN DAM, J.C. (Ed.). **Unsaturated-zone modeling: Progress, challenges, and applications**. Dordrecht: Kluwer Academic Publishers, 2004. p. 95–141.

FRIED, M.; SHAPIRO, R.E. Soil-plant relationships in ion uptake. **Annual Review of Plant Physiology**, Palo Alto, v. 12, n. 1, p. 91–112, 1961.

GARDNER, W.R. Dynamic aspects of soil-water availability to plants. **Annual review of plant physiology**, Palo Alto, v. 16, n. 1, p. 323–342, 1965.

HOMAEE, M. **Root water uptake under non-uniform transient salinity and water stress**. 173 p. Thesis (PhD) — Wageningen University, 1999.

KELLY, J.M.; BARBER, S.A. Magnesium uptake kinetics in loblolly pine seedlings. **Plant and soil**, Dordrecht, v. 134, n. 2, p. 227–232, 1991.

KOCHIAN, L.V.; LUCAS, W.J. Potassium transport in corn roots i. resolution of kinetics into a saturable and linear component. **Plant Physiology**, Rockville, v. 70, n. 6, p. 1723–1731, 1982.

LAMBERS, H.; CHAPIN III, F.S.; PONS, T.L. Plant water relations. In: _____. **Plant Physiological Ecology**. New York: Springer, 2008. Chapter 3, p. 163–223.

LUX, A.; MARTINKA, M.; VACULÍK, M.; WHITE, P.J. Root responses to cadmium in the rhizosphere: a review. **Journal of Experimental Botany**, Oxford, v. 62, n. 1, p. 21–37, 2011.

MACHADO, C.T.d.T.; FURLANI, Â.M.C. Kinetics of phosphorus uptake and root morphology of local and improved varieties of maize. **Scientia Agricola**, São Paulo, v. 61, n. 1, p. 69–76, 2004.

MCKNIGHT, P.E.; NAJAB, J. Mann-whitney u test. In: WEINER, I.B.; E, C.W. (Ed.). **The Corsini Encyclopedia of Psychology**. Hoboken: Wiley Online Library, 2010. p. 960–961.

MOUAT, M.C.H. Phosphate uptake from extended soil solutions by pasture plants. **New Zealand Journal of Agricultural Research**, Wellington, v. 26, n. 4, p. 483–487, 1983.

MUALEM, Y. A new model for predicting the hydraulic conductivity of unsaturated porous media. **Water resources research**, Washington, v. 12, n. 3, p. 513–522, 1976.

NOBEL, P.S. **Physicochemical and environmental plant physiology**. 2 ed. San Diego: Academic press, 1999. 489 p.

NYE, P.H.; MARRIOTT, F.H.C. A theoretical study of the distribution of substances around roots resulting from simultaneous diffusion and mass flow. **Plant and Soil**, Dordrecht, v. 30, n. 3, p. 459–472, 1969.

NYE, P.H.; TINKER, P.B. **Solute movement in the soil-root system**. Berkeley: University of California Press, 1977. 325 p.

PARRA, M.A.; ROMERO, G.C. On the dependence of salt tolerance of beans (phaseolus vulgaris l.) on soil water matric potentials. **Plant and Soil**, Dordrecht, v. 56, n. 1, p. 3–16, 1980.

RENGEL, Z. Mechanistic simulation models of nutrient uptake: a review. **Plant and Soil**, Dordrecht, v. 152, n. 2, p. 161–173, 1993.

ROBINSON, D. The responses of plants to non-uniform supplies of nutrients. **New Phytologist**, Malden, v. 127, n. 4, p. 635–674, 1994.

ROOSE, T. **Mathematical model of plant nutrient uptake**. 226 p. Thesis (PhD) — Oxford University, Mathematical Institute, 2000.

ROOSE, T.; FOWLER, A.C.; DARRAH, P.R. A mathematical model of plant nutrient uptake. **Journal of mathematical biology**, New York, v. 42, n. 4, p. 347–360, 2001.

ROOSE, T.; KIRK, G.J.D. The solution of convection–diffusion equations for solute transport to plant roots. **Plant and soil**, Dordrecht, v. 316, n. 1-2, p. 257–264, 2009.

ROSS, G.J.S. Use of non-linear regression methods in crop modelling. In: ROSE, D.A.; CHARLES-EDWARDS, D.A. (Ed.). **Mathematics and plant physiology**. London: Academic Press, 1981. p. 253–267.

SADANA, U.S.; SHARMA, P.; ORTIZ, N. C.; SAMAL, D.; CLAASSEN, N. Manganese uptake and mn efficiency of wheat cultivars are related to mn-uptake kinetics and root growth. **Journal of Plant Nutrition and Soil Science**, Weinheim, v. 168, n. 4, p. 581–589, 2005.

SCHRÖDER, N.; JAVAUX, M.; VANDERBORGHT, J.; STEFFEN, B.; VEREECKEN, H. Effect of root water and solute uptake on apparent soil dispersivity: A simulation study. **Vadose Zone Journal**, Madison, v. 11, n. 3, p. 1–14, 2012.

SEELING, B.; CLAASSEN, N. A method for determining michaelis-menten kinetic parameters of nutrient uptake for plants growing in soil. **Zeitschrift für Pflanzenernährung und Bodenkunde**, Weinheim, v. 153, n. 5, p. 301–303, 1990.

SEPASKHAH, A.R.; BOERSMA, L. Shoot and root growth of wheat seedlings exposed to several levels of matric potential and nacl-induced osmotic potential of soil water. **Agronomy Journal**, Madison, v. 71, n. 5, p. 746–752, 1979.

SHALHEVET, J.; HSIAO, T.C. Salinity and drought. **Irrigation Science**, New York, v. 7, n. 4, p. 249–264, 1986.

SHI, J.; BEN-GAL, A.; YERMIYAHU, U.; WANG, L.; ZUO, Q. Characterizing root nitrogen uptake of wheat to simulate soil nitrogen dynamics. **Plant and soil**, Dordrecht, v. 363, n. 1-2, p. 139–155, 2013.

SIDDIQI, M.Y.; GLASS, A.D.; RUTH, T.J.; RUFTY, T.W. Studies of the uptake of nitrate in barley i. kinetics of 13no3-influx. **Plant Physiology**, Rockville, v. 93, n. 4, p. 1426–1432, 1990.

SILBERBUSH, M.; ESHEL, A.; LYNCH, J. Nutrient uptake and root system architecture modeling. In: ESHEL, A.; BEECKMAN, T. (Ed.). **Plant roots: the hidden half**. Boca Raton: CRC Press, 2013. p. 390–403.

ŠIMUNEK, J.; HOPMANS, J.W. Modeling compensated root water and nutrient uptake. **Ecological modelling**, Baltimore, v. 220, n. 4, p. 505–521, 2009.

ŠIMÙNEK, J.; ŠEJNA, M.; VAN GENUCHTEN, M.T. The hydrus software package for simulating the two-and three-dimensional movement of water, heat, and multiple solutes in variably-saturated media. **Technical manual**, v. 1, n. 1, p. 241, 2006.

SOMMA, F.; HOPMANS, J.W.; CLAUSNITZER, V. Transient three-dimensional modeling of soil water and solute transport with simultaneous root growth, root water and nutrient uptake. **Plant and Soil**, Dordrecht, v. 202, n. 2, p. 281–293, 1998.

TINKER, P.; NYE, P. **Solute Movement in the Rhizosphere**. [S.l.]: Oxford University Press, 2000. (Topics in sustainable agronomy).

VALLEJO, A.J.; PERALTA, M.L.; SANTA-MARIA, G.E. Expression of potassium-transporter coding genes, and kinetics of rubidium uptake, along a longitudinal root axis. **Plant, Cell & Environment**, Malden, v. 28, n. 7, p. 850–862, 2005.

VAN DAM, J.C.; FEDDES, R.A. Numerical simulation of infiltration, evaporation and shallow groundwater levels with the richards equation. **Journal of Hydrology**, Amsterdam, v. 233, n. 1, p. 72–85, 2000.

VAN DAM, J.C.; GROENENDIJK, P.; HENDRIKS, R.F.A.; KROES, J.G. Advances of modeling water flow in variably saturated soils with swap. **Vadose Zone Journal**, Madison, v. 7, n. 2, p. 640–653, 2008.

VAN GENUCHTEN, M.T. A closed-form equation for predicting the hydraulic conductivity of unsaturated soils. **Soil science society of America journal**, Madison, v. 44, n. 5, p. 892–898, 1980.

VON NEUMANN, J.; RICHTMYER, R.D. A method for the numerical calculation of hydrodynamic shocks. **Journal of applied physics**, Melville, v. 21, n. 3, p. 232–237, 1950.

WANG, M.Y.; SIDDIQI, M.Y.; RUTH, T.J.; GLASS, A.D. Ammonium uptake by rice roots (ii. kinetics of 13nh4+ influx across the plasmalemma). **Plant physiology**, Rockville, v. 103, n. 4, p. 1259–1267, 1993.

WÖSTEN, J.H.M.; VEERMAN, G.J.; GROOT, W.J.M. D.; STOLTE, J. Waterretentie- en doorlatendheidskarakteristieken van boven-en ondergronden in nederland: de staringsreeks. Alterra, Research Instituut voor de Groene Ruimte, 2001.

YEROKUN, O.A.; CHRISTENSON, D.R. Relating high soil test phosphorus concentrations to plant phosphorus uptake. **Soil Science Society of America Journal**, Madison, v. 54, n. 3, p. 796–799, 1990.

APPENDICES

APPENDIX A - Derivation of microscopic model root related equations

The derivation of Equation (5), here repeated

$$R = \frac{1}{\pi {r_m}^2} \,,$$

can be done by verifying that the root length density (R) is the sum of all root lengths (z) per volume of soil (V_{soil}). If we consider that the arrangement showed in Figure 2 has n roots, the root length (L) is simply $z_1 + z_2 + ... + z_n$. Similarly, the soil surface area occupied by the plant (A_p) is the sum of the soil surface areas of the circles with radius r_m (A_s), or $A_p = A_{s_1} + A_{s_2} + ... + A_{s_n}$. Therefore, mathematically:

$$R = \frac{L}{V_{soil}} = \frac{L}{A_p z} = \frac{z_1 + z_2 + ... + z_n}{(A_{s_1} + A_{s_2} + ... + A_{s_n})z}. \tag{73}$$

All the cylinders have the same depth and the same radius, thus $z_1 = z_2 = ... = z_n = z$ and $A_{s_1} = A_{s_2} = ... = A_{s_n} = A_s$. Knowing that $A_s = \pi {r_m}^2$, Equation (73) can be rewritten as

$$R = \frac{nz}{nA_s z} = \frac{1}{A_s} \Rightarrow R = \frac{1}{\pi {r_m}^2} \quad \text{q.e.d.} \tag{74}$$

To derive Equation (4)

$$r_m = \sqrt{\frac{A_p z}{\pi L}} \,,$$

we start by solving Equation (74) for r_m

$${r_m}^2 = \frac{1}{\pi R} \,, \tag{75}$$

so that r_m is a function of R. Analysing Equation (75), and with the help of Figure 2, it is easy to notice that an increase in root length density implies that there are more roots in the same soil volume and, therefore, the space between the roots is diminished. Hence, we can replace R in Equation (75) by its relation between L, z and A_p from Equation (73) to have:

$${r_m}^2 = \frac{1}{\pi \frac{L}{A_p z}} = \frac{A_p z}{\pi L} \Rightarrow r_m = \sqrt{\frac{A_p z}{\pi L}} \quad \text{q.e.d.} \tag{76}$$

With Equations (75) and (76) we have basic relationships of the parameters that can be arranged to find expressions for any of them, as long we have enough measured parameters. Thus, for a known value of R, r_m can be calculated using Equation (75), and L by solving Equation (76) for L. The former yields

$$r_m = \frac{1}{\sqrt{\pi R}} \,,$$

which is the Equation (1), and the later yields

$$L = \frac{A_p z}{\pi {r_m}^2},$$

which is the Equation (2).

As mentioned in Section 3.1, when there is no root length density data available (or other parameter that can lead to it), it is necessary to measure some root and soil characteristics of an experimental set to find parameters such as L, r_m or R. By finding one of them, it is possible to have the others through the relations presented in the previous equations of this appendix. Here, it is demonstrated the development of Equation (3):

$$L = \frac{d_s A_p z - m_s}{d_s \pi \overline{r_0}^2}$$

where d_s is the soil density, m_s is the soil mass and $\overline{r_0}$ is the average root radius. All parameters are relatively easy to be measured. $\overline{r_0}$ can be troublesome but there are methodologies to measure it properly. d_s and m_s are routine in soil physics laboratories and A_p is known. The total volume of a one-plant experimental parcel is the sum of soil and root volumes. Since it is difficult to measure the root volume, it can be estimated by difference between total and soil volumes. The first can be found by multiplying plant area by root depth and the later by the relation between soil volume, mass and density. Hence, volume of roots can be calculated as follows:

$$V_t = V_r + V_s \Rightarrow V_r = V_t - V_s = A_p z - \frac{m_s}{d_s} \tag{77}$$

Also, as roots are considered cylinders, their volume can be calculated as the volume of a cylinder:

$$V_r = \pi \overline{r_0}^2 L \tag{78}$$

The unknown is L, all other parameters are measured. Relating the two V_r equations, we can, thus, solve for L:

$$A_p z - \frac{m_s}{d_s} = \pi \overline{r_0}^2 L \Rightarrow L = \left(A_p z - \frac{m_s}{d_s} \right) \frac{1}{\pi \overline{r_0}^2} \Rightarrow L = \frac{d_s A_p z - m_s}{d_s \pi \overline{r_0}^2} \quad \text{q.e.d.} \tag{79}$$

APPENDIX B - Algorithm used to solve Equation (23)

Applying Equation (23) to each segment i, the values of H_i^{j+1} is found by solving the tridiagonal matrix as follows

$$\begin{bmatrix} \beta_1 & \gamma_1 & & & & \\ \alpha_2 & \beta_2 & \gamma_2 & & & \\ & \alpha_3 & \beta_3 & \gamma_3 & & \\ & & \ddots & \ddots & \ddots & \\ & & & \alpha_{n-1} & \beta_{n-1} & \gamma_{n-1} \\ & & & & \alpha_n & \beta_n \end{bmatrix} \begin{bmatrix} H_1^{j+1} \\ H_2^{j+1} \\ H_3^{j+1} \\ \vdots \\ H_{n-1}^{j+1} \\ H_n^{j+1} \end{bmatrix} = \begin{bmatrix} g_1 \\ g_2 \\ g_3 \\ \vdots \\ g_{n-1} \\ g_n \end{bmatrix} \tag{80}$$

in which $H_n = h_n + h_{\pi n}$ and $h_{\pi n}$ is the osmotic head of the last time step; α_i, β_i, γ_i and g_i are defined as described in the following.

1. Intermediate segments ($i = 2$ to $i = n - 1$):

$$\alpha_i = -\frac{t^{j+1} - t^j}{r_i(r_i - r_{i-1})\Delta r_i} r_{i-1/2} K_{i-1/2}^j \tag{81}$$

$$\beta_i = C_{wi}^{j+1,p-1} + \frac{t^{j+1} - t^j}{r_i(r_i - r_{i-1})\Delta r_i} r_{i-1/2} K_{i-1/2}^j + \frac{t^{j+1} - t^j}{r_i(r_{i+1} - r_i)\Delta r_i} r_{i+1/2} K_{i+1/2}^j \tag{82}$$

$$\gamma_i = -\frac{t^{j+1} - t^j}{r_i(r_{i+1} - r_i)\Delta r_i} r_{i+1/2} K_{i+1/2}^j \tag{83}$$

$$g_i = C_{wi}^{j+1,p-1} H_i^{j+1,p-1} - \theta_i^{j+1,p-1} + \theta_i^j \tag{84}$$

2A. Root segment ($i = 1$) with flux boundary condition, applied while $H_1 > H_{lim}$, i.e., when transpiration meets potential transpiration demand:

$$\beta_1 = C_{w1}^{j+1,p-1} + \frac{t^{j+1} - t^j}{r_1(r_2 - r_1)\Delta r_1} r_{1+1/2} K_{1+1/2}^j \tag{85}$$

$$\gamma_1 = -\frac{t^{j+1} - t^j}{r_1(r_2 - r_1)\Delta r_1} r_{1+1/2} K_{1+1/2}^j \tag{86}$$

$$g_1 = C_{w1}^{j+1,p-1} H_1^{j+1,p-1} - \theta_1^{j+1,p-1} + \theta_1^j - \frac{r_0 q_0 (t^{j+1} - t^j)}{r_1 \Delta r_1} \tag{87}$$

where $q_0 = \dfrac{T_p}{2\pi r_o R z}$.

2B. Root segment ($i = 1$) with head boundary condition, applied while $H_1 = H_{lim}$, i.e., when transpiration is less than potential transpiration demand:

$$\beta_1 = C_{w1}^{j+1,p-1} + \frac{t^{j+1} - t^j}{r_1(r_1 - r_0)\Delta r_1} r_{1/2} K_{1/2}^j + \frac{t^{j+1} - t^j}{r_1(r_2 - r_1)\Delta r_1} r_{1+1/2} K_{1+1/2}^j \tag{88}$$

$$\gamma_1 = -\frac{t^{j+1} - t^j}{r_1(r_2 - r_1)\Delta r_1} r_{1+1/2} K_{1+1/2}^j \tag{89}$$

$$g_1 = C_{w1}^{j+1,p-1} H_1^{j+1,p-1} - \theta_1^{j+1,p-1} + \theta_1^j + \frac{t^{j+1} - t^j}{r_1(r_1 - r_0)\Delta r_1} r_{1/2} K_{1/2}^j H_{lim} \tag{90}$$

3. Outer segment ($i = n$):

$$\alpha_n = -\frac{t^{j+1} - t^j}{r_n(r_n - r_{n-1})\Delta r_n} r_{n-1/2} K^j_{n-1/2} \tag{91}$$

$$\beta_n = C_{w_n}^{j+1,p-1} + \frac{t^{j+1} - t^j}{r_n(r_n - r_{n-1})\Delta r_n} r_{n-1/2} K^j_{n-1/2} \tag{92}$$

$$g_n = C_{w_n}^{j+1,p-1} H_n^{j+1,p-1} - \theta_n^{j+1,p-1} + \theta_n^j \tag{93}$$

The value of pressure head h is calculated and added to H using the value of osmotic head (h_π) from the previous time step. The values of h_π are calculated and then the values of H are updated in the next time step. The process repeats until the values of updated H converge to H from the previous time step.

APPENDIX C - Finding C_{lim}, C_2 and linearizing MM equation

According to the assumptions made over the MM equation (described in Chapter 4), the diffusive and convective contributions for the uptake are driven by active and passive processes. It is shown in Figure 30 the two limiting concentrations (C_{lim} and C_2), and the non-linear (Figure 30a) and linear (Figure 30b) uptake functions.

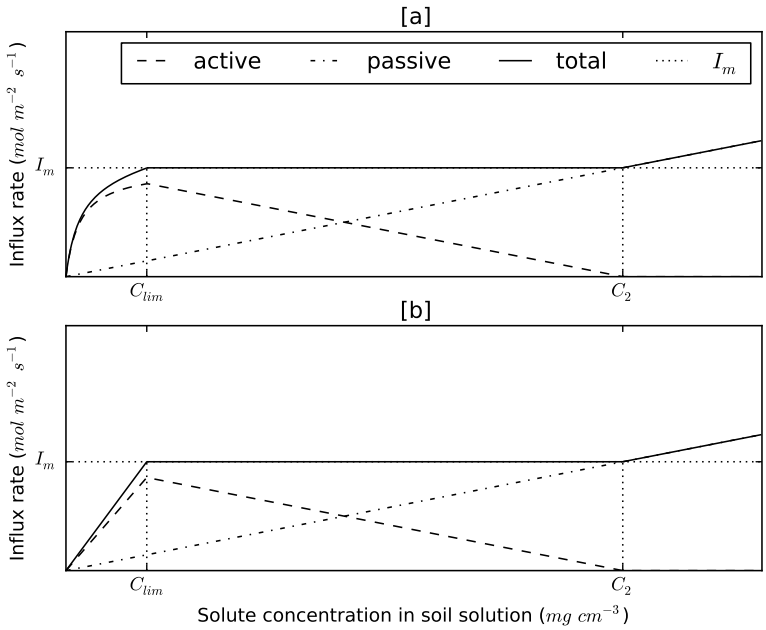

Figure 30 - Uptake (influx) rate as a function of concentration in soil water for [a] non-linear case and [b] linear case. C_{lim} is the limiting concentration in which the uptake is limited by the solute flux and C_2 is the concentration where the uptake is governed by convective flow only

In the linearized equation, the slope β of the total uptake line (continuous line), for concentration values smaller than C_{lim}, can be found by the relation I_m/C_{lim}, since the line starts at the origin of the Cartesian coordinates system:

$$\beta = \frac{I_m}{C_{lim}}. \tag{94}$$

According to our assumptions, at values smaller than C_{lim} the solute uptake is concentration dependent and the uptake is smaller than the plant demand I_m. Additionally, for values greater than C_2, the solute uptake occurs due to the mass transport by water flow only, *i.e.* active uptake is zero and the overall uptake is passive.

Therefore, C_{lim} can be calculated by setting the value of solute flux density at the root surface (q_{s0}, Equation (29.1)) to I_m and C_0 to C_{lim}:

$$I_m = \frac{I_m C_{lim}}{K_m + C_{lim}} + q_0 C_{lim}\ . \tag{95}$$

Solving Equation (95) for C_{lim}, we find it as the positive value of:

$$C_{lim} = -\frac{K_m \pm \left({K_m}^2 + 4 I_m K_m / q_0\right)^{1/2}}{2} \tag{96}$$

Substitution of Equation (96) into (94), the slope of total uptake β can be defined as the positive value of:

$$\beta = \frac{I_m}{C_{lim}} = -\frac{2 I_m}{K_m \pm \left({K_m}^2 + 4 I_m K_m / q_0\right)^{1/2}}. \tag{97}$$

At concentration values greater than C_2, the solute uptake is driven only by mass flow of water and the active uptake is zero. Thus, the first term of the right-hand-side of Equation (29.1) is zero and C_2 can be found by setting q_{s0} to I_m and C_0 to C_2:

$$I_m = q_0 C_2 \Rightarrow C_2 = \frac{I_m}{q_0} \tag{98}$$

The partitioning between active (αC_0) and passive ($q_0 C_0$) uptake is calculated by difference, as the values of total uptake (βC_0) and passive uptake is always known:

$$\begin{aligned} &q_{s0} = (\text{active slope} + \text{passive slope})\, C_0 = \beta\, C_0; \\ &\text{passive slope} = q_0; \\ &\text{active slope} = \beta - q_0 = \alpha; \\ &q_{s0} = (\alpha + q_0)\, C_0. \end{aligned} \tag{99}$$

The equation (99) is, therefore, the linearization of equation (29.1), and it is used in the piecewise equation (29) for values of concentration smaller than C_{lim} and greater than C_2 (with $\alpha = 0$).

APPENDIX D - Flowcharts algorithms to solve combined water and solute transport and uptake

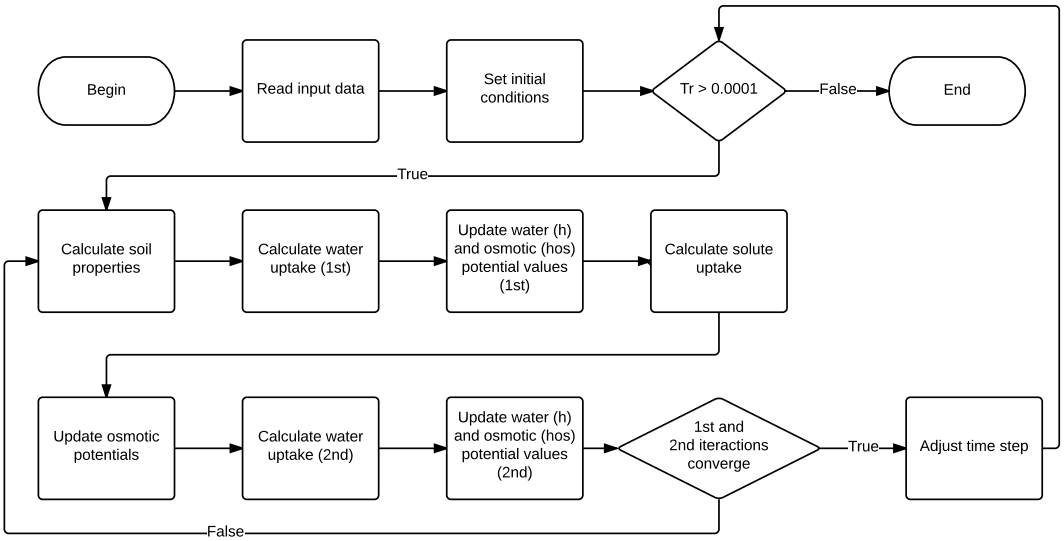

Figure 31 - General algorithm to solve combined water and solute transport in soil and uptake by the plant

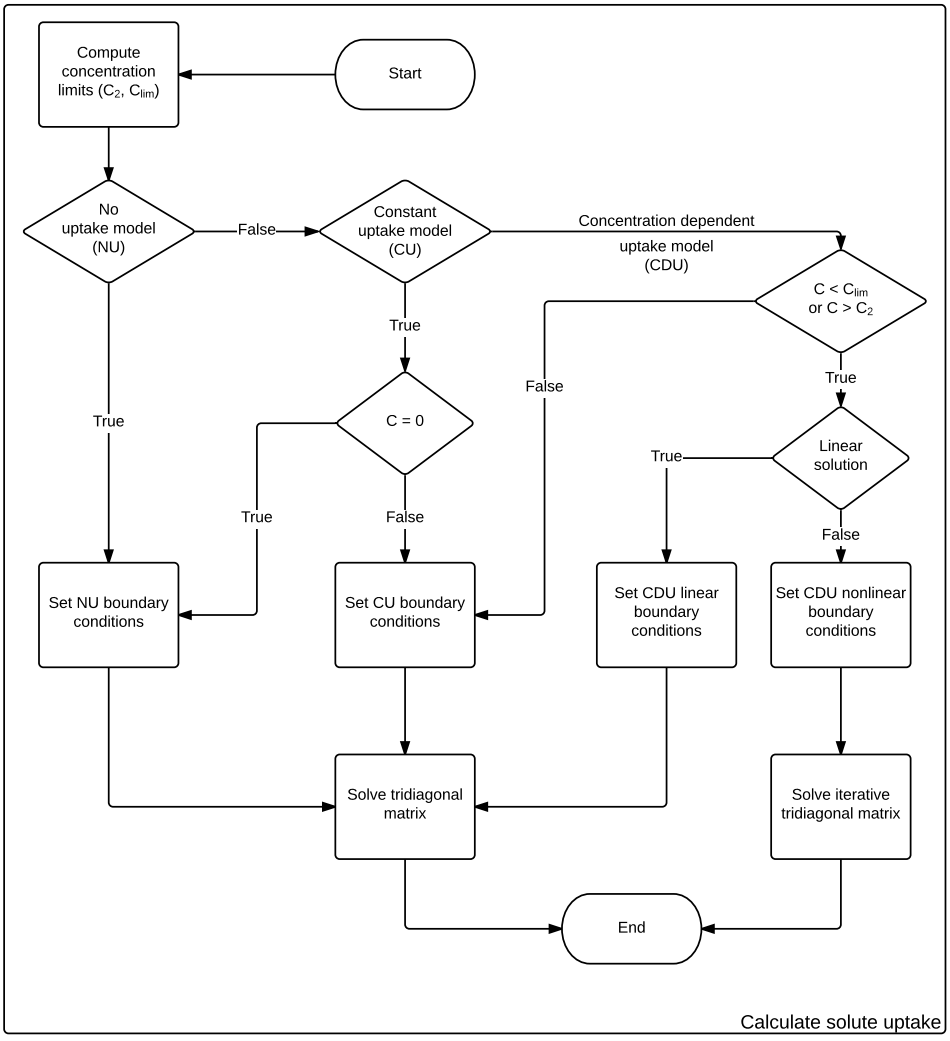

Figure 32 - Detail of *Calculate solute uptake* procedure from the general algorithm